4 Fiber polytopes

Que mes claviers seront usés
D'avoir osé
Toujours vouloir tout essayer
Et recommencer
Là où le monde a commencé
– Michel Berger, *Le Paradis Blanc*

4.1 Preliminaries on fiber polytopes

In the following, we give a very brief introduction to fiber polytopes, secondary polytopes and π-coherent subdivisions arising from a polytope projection $\pi : \mathsf{P} \to \mathsf{Q}$. For an instructive and illustrated presentation of the subject, we advise the reader to look at [Zie98, Chapter 9], a more in depth explanation can be found in [ALRS00, Section 2] and [LRS10, Chapter 9.1], and the original articles [BS92] (for fiber polytopes) and [GKZ90, GKZ91] (for secondary polytopes) give the details of the proofs.

Definition 4.1. A *polytope projection* is a couple (P, π) where $\mathsf{P} \subset \mathbb{R}^d$ is a polytope and $\pi : \mathbb{R}^d \to \mathbb{R}^{d'}$ is a projection. When dimensions are obvious or irrelevant, we usually denote such a projection by $\pi : \mathsf{P} \to \mathsf{Q}$ assuming that $\mathsf{Q} := \pi(\mathsf{P})$.

In order to define fiber polytopes, we need to introduce (coherent) subdivisions. The notion of a complex is widely spread in mathematics, and we have already seen an instance of them, as fans are complexes. Here, we only focus on polyhedral complexes.

Definition 4.2. A *polyhedral complex* $\mathcal{C}$ is a collection of polytopes such that if $\mathsf{P} \in \mathcal{C}$, then all the faces of P are in $\mathcal{C}$, and if $\mathsf{P}, \mathsf{Q} \in \mathcal{C}$, then the intersection $\mathsf{P} \cap \mathsf{Q}$ is a face of both P and Q.

A *subdivision* of a polytope Q is a polyhedral complex $\mathcal{C}$ such that $\bigcup_{\mathsf{P} \in \mathcal{C}} \mathsf{P} = \mathsf{Q}$.

Definition 4.3. For a polytope projection $\pi : \mathsf{P} \to \mathsf{Q}$, a *$\pi$-induced subdivision* of Q is a subdivision $\pi(\mathcal{F})$ of Q where:
(i) $\pi(\mathcal{F}) = \{\pi(F) \ ; \ F \in \mathcal{F}\}$ for $\mathcal{F}$ a family of faces of P.
(ii) for $F, F' \in \mathcal{F}$, if $\pi(F) \subseteq \pi(F')$, then $F = F' \cap \pi^{-1}(\pi(F))$.

The set of π-induced subdivisions is ordered by refinement, forming the *Baues poset*: $\pi(\mathcal{F}_1) \preccurlyeq \pi(\mathcal{F}_2)$ when every polytope of $\pi(\mathcal{F}_2)$ is a union of polytopes of $\pi(\mathcal{F}_1)$. More conveniently, as $\mathcal{F}$ can be recovered from the knowledge of $\pi(\mathcal{F})$ (see [Zie98, Chapter 9]), one has that $\pi(\mathcal{F}_1) \preccurlyeq \pi(\mathcal{F}_2)$ if and only if $\bigcup_{F \in \mathcal{F}_1} F \subseteq \bigcup_{F \in \mathcal{F}_2} F$.

By convention, the empty family will be considered a π-induced subdivision. It is the minimal element of the Baues poset. Note that even if they are called *subdivisions*, the π-induced subdivisions are better thought of not as subdivisions of Q, but as polyhedral complexes that live in P (and whose projection by π is a subdivision of Q). Among π-induced subdivisions, some appear as special (regular) subdivisions, we follow here the reformulation of [Zie98].

Definition 4.4. ([Zie98, definition 9.2]) Let $\pi : \mathsf{P} \to \mathsf{Q}$ be a polytope projection with $\dim \mathsf{P} = d$ and $\dim \mathsf{Q} = d'$. For $\boldsymbol{\omega} \in \mathbb{R}^d$, define $\pi^{\boldsymbol{\omega}} : \mathbb{R}^d \to \mathbb{R}^{d'+1}$ by

$$\pi^{\boldsymbol{\omega}}(\boldsymbol{x}) = \begin{pmatrix} \pi(\boldsymbol{x}) \\ \langle \boldsymbol{\omega}, \boldsymbol{x} \rangle \end{pmatrix}$$

The family of lower faces[13] of $\pi^{\boldsymbol{\omega}}(\mathsf{P})$ projects down to Q by forgetting the last coordinate, giving rise to a π-induced subdivision of Q. The π-induced subdivisions of this form are called *π-coherent subdivisions*, and form a sub-poset of the Baues poset: the *lattice of π-coherent subdivisions*.

We say that $\boldsymbol{\omega}$ *captures* the subdivision.

[13] A face is a lower face when its normal cone contains a vector with a negative last coordinate.

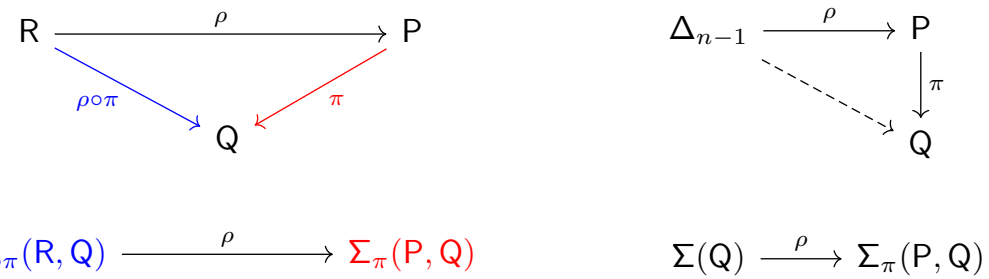

Figure 55: (Left) A projection $\rho : \mathsf{R} \to \mathsf{P}$ induces a projection between the fiber polytopes of R and P for their projections onto Q. Note that as ρ and π are projection $|V(\mathsf{R})| \geq |V(\mathsf{P})| \geq |V(\mathsf{Q})|$. (Right) If $n = |V(\mathsf{Q})|$, then $\Sigma_\pi(\mathsf{P}, \mathsf{Q})$ is a projection of $\Sigma(\mathsf{Q})$ when $|V(\mathsf{P})| = |V(\mathsf{Q})| = n$.

Note that when $\boldsymbol{\omega}$ is generic with respect to P, then the associated π-coherent subdivision is a finest π-coherent subdivision in the sense that it covers the empty subdivision in the Baues poset.

The fiber polytope has several (equivalent) definitions. In the present thesis, even though the formal definition is given here, we will not use the realization of the fiber polytope, but only focus on the characterization of its face lattice given in the following Theorem 4.6.

Definition 4.5. For a polytope projection $\pi : \mathsf{P} \to \mathsf{Q}$, a *section* of P is a continuous map $\gamma : \mathsf{Q} \to \mathsf{P}$ satisfying $\pi \circ \gamma = \mathrm{id}_\mathsf{Q}$. The *fiber polytope* $\Sigma_\pi(\mathsf{P}, \mathsf{Q})$ for the projection $\pi : \mathsf{P} \to \mathsf{Q}$ is defined by:

$$\Sigma_\pi(\mathsf{P}, \mathsf{Q}) = \left\{ \frac{1}{\mathrm{vol}(\mathsf{Q})} \int_\mathsf{Q} \gamma(\boldsymbol{x}) \mathrm{d}\boldsymbol{x} \ ; \ \gamma \text{ section of } \mathsf{P} \right\}$$

Theorem 4.6. ([BS92, Corollary 1.4]). *For a polytope projection $\pi : \mathsf{P} \to \mathsf{Q}$, the fiber polytope $\Sigma_\pi(\mathsf{P}, \mathsf{Q})$ is a polytope and its face lattice is (isomorphic to) the lattice of π-coherent subdivisions of Q.*

Note that $\Sigma_\pi(\mathsf{P}, \mathsf{Q})$ is of dimension $\dim(\mathsf{P}) - \dim(\mathsf{Q})$, though embedded in $\mathbb{R}^{\dim(\mathsf{P})}$.

The construction of fiber polytopes through Definition 4.5 is cumbersome for numerical computations and drawings. Fortunately, the following theorem provides a description of fiber polytopes as a **finite** Minkowski sum.

Theorem 4.7. ([BS92, Theorem 1.5]). *For the polytope projection $\pi : \mathsf{P} \to \mathsf{Q}$, consider the subdivision of Q defined as the common refinement of all $\pi(\mathsf{F})$ for F a face of P. For each maximal cell C of this subdivision, we denote $\boldsymbol{b}_\mathsf{C}$ the barycenter (or centroid) of C. Then:*

$$\Sigma_\pi(\mathsf{P}, \mathsf{Q}) = \frac{1}{\mathrm{vol}(\mathsf{Q})} \sum_{\mathsf{C} \text{ maximal cells}} \mathrm{vol}(\mathsf{C}) \ \pi^{-1}(\boldsymbol{b}_\mathsf{C})$$

Even though an adequate construction of a category of polytopes is still lacking, fiber polytopes have a categorical flavor. Indeed, if one would construct a category **Pol** in which objects are polytopes, and morphisms are (surjective) projections between polytopes, then the map $(\pi : \mathsf{P} \to \mathsf{Q}) \mapsto \Sigma_\pi(\mathsf{P}, \mathsf{Q})$ would resemble a functor from the category of morphisms of **Pol** to **Pol** itself. The commutative diagram of Figure 55(Left) indicates how the (categorical) cone over Q would be sent to **Pol** by this functor. Notably, the following proposition guaranties fiber polytopes are well-behaved with respect to projections:

Proposition 4.8. ([BS92, Lemma 2.3]). *For two polytopes projections $\rho : \mathsf{R} \to \mathsf{P}$ and $\pi : \mathsf{P} \to \mathsf{Q}$, one has:*

$$\Sigma_\pi(\mathsf{P}, \mathsf{Q}) = \rho\big(\Sigma_{\pi\circ\rho}(\mathsf{P}, \mathsf{R})\big)$$

Among all fiber polytopes, some are very special. For instance, when projecting a simplex onto a polytope, the finest π-coherent subdivisions are then in bijection with all regular triangulations of P. This motivates the construction of the following universal object.

Definition 4.9. Consider the standard simplex $\Delta_n = \text{conv}(\boldsymbol{e}_1, ..., \boldsymbol{e}_n) \subset \mathbb{R}^n$ and a polytope P of dimension d with vertices $(\boldsymbol{v}_1, ..., \boldsymbol{v}_n)$. Let $\pi : \mathbb{R}^n \to \mathbb{R}^d$ be the projection defined by $\pi(\boldsymbol{e}_i) = \boldsymbol{v}_i$. Then the dilate of the fiber polytope $\Sigma(\mathsf{P}) := (d+1)\text{vol}(\mathsf{P})\Sigma_\pi(\Delta_n, \mathsf{P})$ is called the *secondary polytope of* P. The vertices of $\Sigma(\mathsf{P})$ are in bijection with the set of regular triangulations of P.

In particular, if P and Q share the same number n of vertices, then there exists a polytope projection $\rho : \Delta_{n-1} \to \mathsf{P}$, see Figure 55(Right). In this setting, the previous proposition ensures:

Corollary 4.10. *If* P *and* Q *share the same number* n *of vertices, then* $\Sigma_\pi(\mathsf{P}, \mathsf{Q})$ *arises as a projection of the secondary polytope of* Q*, i.e. there exists a projection* ρ *such that:*

$$\Sigma_\pi(\mathsf{P}, \mathsf{Q}) = \rho\big(\Sigma(\mathsf{Q})\big)$$

This corollary is only a glint of the more general theory of secondary polytopes. They were defined to study triangulations of any points configuration. We limit ourselves to secondary polytopes of polytopes (*i.e.* points configuration in convex position), but the interested reader is referred to the original papers of Gelfand, Kapranov and Zelevinsky [GKZ90, GKZ91] for a global presentation. In particular, it is important to keep in mind that any fiber polytope is a projection of a secondary polytope of a points configuration, but only fiber polytopes for projections that retain the number of vertices are projections of secondary polytopes of polytopes.

4.2 Monotone path polytopes of the hypersimplices

This section is a work on my own on a question originally asked by Alex Black and a conjecture from Jesús De Loera. An article is in preparation.

After their introduction by Billera and Sturmfels in [BS92], fiber polytopes have received a lot of attention. Especially, the fiber polytope for the projection of a polytope P onto a segment encapsulates the combinatorics of monotone paths on P. For this reason, it is called the *monotone path polytope* of P [Ath99, AER00, BLL20]. The vertices of the monotone path polytopes are in bijection with the monotone paths that can be followed by a shadow vertex rule. As such, it links the world of linear optimization to the world of triangulations.

This, and the fact that monotone path polytopes stand among the easiest fiber polytopes to compute, have motivated numerous studies on the subject. Especially, the monotone path polytope of a simplex is a cube [BS92], the one of a cube is a permutahedron [BS92, Zie98, Example 9.8], the one of a cyclic polytope is a cyclic zonotope [ALRS00], the one of a cross-polytope is the signohedron [BL21], and the one of a S-hypersimplex is a permutahedron [MSS20].

However, the monotone path polytopes of the hypersimplices have not yet been explored. The (n,k)-*hypersimplex* $\Delta(n,k)$ can be equivalently defined as the section of the standard cube by the hyperplane $\{\boldsymbol{x} \in \mathbb{R}^n \ ; \ \sum_i x_i = k\}$, or as the convex hull of the $(0,1)$-vectors with k ones and $n-k$ zeros [Zie98, Example 0.11]. Hypersimplices appear as usual examples of various classes of examples ranging from generalized permutahedra [Pos09] to matroid polytopes of uniform matroids [ABD10], and alcove polytopes [LP07]. Moreover, triangulations of the second hypersimplex $\Delta(n,2)$ can be interpreted as through toric ideals of the complete graph [DLST95].

In the present section, we begin with a general introduction to monotone path polytopes (Section 4.2.1), and then examine the monotone path polytopes of hypersimplices, especially their vertices. We give a necessary criterion for a monotone path on $\Delta(n,k)$ to appear as a vertex of its monotone path polytope (Section 4.2.2). We prove that this criterion is furthermore sufficient in the case of the second hypersimplex (Section 4.2.3) and give the exact count of the vertices of the monotone path polytope of $\Delta(n,2)$ (Section 4.2.4).

4.2.1 Monotone paths polytopes in general

In general, fiber polytopes are, by construction, complicated to compute, even with the help of Theorem 4.7. As a simple case, fiber polytopes for projections onto a point are trivial, as $\Sigma_\pi(\mathsf{P}, \{\boldsymbol{q}\}) = \mathsf{P}$. Hence, among the first cases one would want to investigate are the fiber polytopes associated to projections onto a 1-dimensional polytope, *i.e.* a segment.

Definition 4.11. For a linear program $(\mathsf{P}, \boldsymbol{c})$, the *monotone path polytope* $\mathsf{M}_{\boldsymbol{c}}(\mathsf{P})$ is the fiber polytope for the projection $\pi_{\boldsymbol{c}} : \boldsymbol{x} \mapsto \langle \boldsymbol{x}, \boldsymbol{c} \rangle$. Denoting the image segment $\mathsf{Q} = \pi_{\boldsymbol{c}}(\mathsf{P}) = \{\langle \boldsymbol{x}, \boldsymbol{c} \rangle \ ; \ \boldsymbol{x} \in \mathsf{P}\}$, one has: $\mathsf{M}_{\boldsymbol{c}}(\mathsf{P}) := \Sigma_{\pi_{\boldsymbol{c}}}(\mathsf{P}, \mathsf{Q})$.

Note that $\mathsf{M}_{\boldsymbol{c}}(\mathsf{P})$ has dimension $\dim(\mathsf{P}) - 1$ but is embedded in $\mathbb{R}^{\dim(\mathsf{P})}$.

The monotone path polytope, though arising from a fiber polytope point of view, is deeply linked to linear programming. Indeed, fix a polytope $\mathsf{P} \subset \mathbb{R}^d$, and consider a finest $\pi_{\boldsymbol{c}}$-coherent subdivision $\mathcal{F}$ of P. By Definition 4.4, this amounts to taking a generic $\boldsymbol{\omega} \in \mathbb{R}^d$ and looking at the polygon $\pi^{\boldsymbol{\omega}}_{\boldsymbol{c}}(\mathsf{P}) = \big\{\big(\langle \boldsymbol{x}, \boldsymbol{c} \rangle, \ \langle \boldsymbol{x}, \boldsymbol{\omega} \rangle\big) \ ; \ \boldsymbol{x} \in \mathsf{P}\big\}$. The family of lower faces of $\pi^{\boldsymbol{\omega}}_{\boldsymbol{c}}(\mathsf{P})$ is at the same time the subdivision $\mathcal{F}$ at stake, and the monotone path followed by the simplex method for the shadow vertex rule with secondary direction $-\boldsymbol{\omega}$. Accordingly, this process gives a clever way to encompass in a polytope the combinatorial behavior of the shadow vertex rule. Note that, whereas pivot rule polytopes (see Section 3.1) cover the behavior the shadow vertex rule[14] has on each vertex of P, the monotone path polytopes only describe the possible coherent *leading paths* on P, that is the coherent paths from the worst vertex to the best, *i.e.* from the vertex $\boldsymbol{v}_{\min} \in V(\mathsf{P})$ minimizing $\langle \boldsymbol{v}, \boldsymbol{c} \rangle$ for $\boldsymbol{v} \in V(P)$ to the vertex $\boldsymbol{v}_{\text{opt}} \in V(\mathsf{P})$ maximizing it. Consequently, the face lattice of the monotone path polytope is the lattice of coherent cellular strings on P.

[14] Technically, max-slope pivot polytopes encompass max-slope pivot rules, a generalization of shadow vertex rules, see Sections 1.3 and 3.1.

Definition 4.12. For a linear program $(\mathsf{P}, \boldsymbol{c})$, a *cellular string* is a sequence $\sigma = (\mathsf{F}_1, \dots, \mathsf{F}_k)$ of faces of P such that $\min(\mathsf{F}_1) = \boldsymbol{v}_{\min}$, $\max(\mathsf{F}_k) = \boldsymbol{v}_{\text{opt}}$, and for all $i \in [k-1]$, $\max(\mathsf{F}_k) = \min(\mathsf{F}_{k+1})$, where minima and maxima are taken with respect to the scalar product against $\boldsymbol{c}$. As $\pi_{\boldsymbol{c}}$-induced subdivisions, cellular strings are ordered by containment of their union. A cellular string σ is *coherent* if there exists $\boldsymbol{\omega} \in \mathbb{R}^d$ such that $\mathsf{F} \in \sigma$ if F is the pre-image by $\pi_{\boldsymbol{c}}$ of a lower face of $\pi_{\boldsymbol{c}}(\mathsf{P})$.

To make the notations consistent and ease the drawings, we will keep for this section the convention of linear programming, saying a cellular string σ is captured by $\boldsymbol{\omega}$ when $\pi^{\boldsymbol{\omega}}_{\boldsymbol{c}}(\sigma)$ is the family of **upper faces** of $\pi^{\boldsymbol{\omega}}_{\boldsymbol{c}}(\mathsf{P})$ (instead of lower faces).

We now present two ways to visualize the monotone path polytope. First of all, Definition 4.4 invites us to focus on the space of all $\boldsymbol{\omega}$ and partition it depending on the coherent cellular strings they yield. Precisely, to a cellular string σ we associate $\mathcal{N}(\sigma) = \{\boldsymbol{\omega} \ ; \ \boldsymbol{\omega} \text{ captures } \sigma\}$. Then $\mathcal{N}(\sigma)$ is a polyhedral cone by linearity of $\pi^{\boldsymbol{\omega}}_{\boldsymbol{c}}$ in $\boldsymbol{\omega}$, and the family $\mathcal{N} = \big(\mathcal{N}(\sigma)\big)_\sigma$ is a fan. This fan is exactly the normal fan of $\mathsf{M}_{\boldsymbol{c}}(\mathsf{P})$. Hence, one can run through all possible $\boldsymbol{\omega} \in \mathbb{R}^d$, orthogonal to $\boldsymbol{c}$ (as all $\boldsymbol{\omega} + \lambda\boldsymbol{c}$ capture the same cellular string for any $\lambda \in \mathbb{R}$), to draw the normal fan of $\mathsf{M}_{\boldsymbol{c}}(\mathsf{P})$, see Figure 56.

This construction gives two interesting properties. On the one hand, it is clear that the normal fan of $\Pi(\mathsf{P}, \boldsymbol{c})$ coarsens the normal fan of $\mathsf{M}_{\boldsymbol{c}}(\mathsf{P})$: the cone associated to a coherent cellular string σ is the union of the cones associated to all coherent multi-arborescences whose leading cellular string is σ, see Figure 57. Consequently:

Proposition 4.13. ([BDLLS22, Proposition 6.2]). *The monotone path polytope $\mathsf{M}_{\boldsymbol{c}}(\mathsf{P})$ is a deformation of the pivot rule polytope $\Pi(\mathsf{P}, \boldsymbol{c})$.*

On the other hand, we have said that for a fixed $\boldsymbol{\omega}$, all $\boldsymbol{\omega}+\lambda\boldsymbol{c}$ for $\lambda \in \mathbb{R}$ capture the same cellular string. Consequently, one can obtain the normal fan of $\mathsf{M}_{\boldsymbol{c}}(\mathsf{P})$ by *projecting* the normal fan of P: to each normal cone $\mathsf{C} \in \mathcal{N}_{\mathsf{P}}$, associate its projection along $\boldsymbol{c}$, namely $\mathsf{C}_\perp := \{\boldsymbol{x} - \frac{\langle \boldsymbol{x}, \boldsymbol{c}\rangle}{\langle \boldsymbol{c}, \boldsymbol{c}\rangle}\boldsymbol{c} \ ; \ \boldsymbol{x} \in \mathsf{C}\}$. Then the common refinement of all $\big(\mathsf{C}_\perp \ ; \ \mathsf{C} \in \mathcal{N}_{\mathsf{P}}\big)$ is the normal fan[15] of $\mathsf{M}_{\boldsymbol{c}}(\mathsf{P})$.

A second way to visualize monotone path polytopes is to use Theorem 4.7. We begin by sorting the vertices of P according to the scalar product against $\boldsymbol{c}$: $V(\mathsf{P}) = \{\boldsymbol{v}_1, \dots, \boldsymbol{v}_n\}$ with $\langle \boldsymbol{v}_i, \boldsymbol{c}\rangle < \langle \boldsymbol{v}_{i+1}, \boldsymbol{c}\rangle$. The maximal cells of the segment $\mathsf{Q} = \pi_{\boldsymbol{c}}(\mathsf{P})$ are then the sub-segments $\mathsf{C}_i := [q_i, q_{i+1}]$ with $q_i = \langle \boldsymbol{v}_i, \boldsymbol{c}\rangle$, and the barycenter (*i.e.* middle) of C_i is trivially $b_i = \frac{q_i + q_{i+1}}{2}$. The monotone path polytope $\mathsf{M}_{\boldsymbol{c}}(\mathsf{P})$ is normally equivalent to the Minkowski sum of sections $\sum_{i=1}^n \pi_{\boldsymbol{c}}^{-1}(b_i)$.

Though exact, this construction is a bit unhandy. Yet, as we will prove in Theorem 4.14, one can forget about centers, as $\mathsf{M}_{\boldsymbol{c}}(\mathsf{P})$ is normally equivalent to $\sum_{i=2}^{n-1} \pi_{\boldsymbol{c}}^{-1}(q_i)$. This gives beautiful pictures, see Figure 58 for the case of the simplex.

Note that, between the two figures, a slight change of perspective happened: to see that the fan constructed in Figures 56 and 57(Left) is the normal fan of the $\mathsf{M}_{\boldsymbol{c}}(\mathsf{P})$ appearing in Figure 58(Right), rotate the latter clockwise slightly so that its bottom left corner fits in the cone with a right angle.

Theorem 4.14. *For a linear program $(\mathsf{P}, \boldsymbol{c})$, denote $V(\mathsf{P}) = \{\boldsymbol{v}_1, \dots, \boldsymbol{v}_n\}$ and $q_i = \langle \boldsymbol{v}_i, \boldsymbol{c}\rangle$ with $q_1 < \dots < q_n$. The monotone path polytope $\mathsf{M}_{\boldsymbol{c}}(\mathsf{P})$ is normally equivalent to the Minkowski sum of sections $\sum_{i=2}^{n-1}\{\boldsymbol{x} \in \mathsf{P} \ ; \ \langle \boldsymbol{x}, \boldsymbol{c}\rangle = q_i\}$.*

Remark 4.15. This theorem is not a new result, but is known in the folklore. We give here a self-contained proof, with the tools developed so far on sections and Minkowski sums, but the reader at ease with the subject shall rather think of it as an exercise on Cayley polytopes.

Proof of Theorem 4.14. For $i \in [1, n]$, we denote $\gamma_i = \{\boldsymbol{x} \in \mathsf{P} \ ; \ \langle \boldsymbol{x}, \boldsymbol{c}\rangle = q_i\}$ the section over q_i and $\zeta_i(\lambda) = \{\boldsymbol{x} \in \mathsf{P} \ ; \ \langle \boldsymbol{x}, \boldsymbol{c}\rangle = \lambda q_i + (1-\lambda)q_{i+1})\}$ for $\lambda \in]0, 1[$.

First, note that the sections γ_1 and γ_n are points, so adding them to $\sum_{i=2}^{n-1} \Gamma_i$ amounts to translating it (without changing its normal equivalence class). For this reason, we will prove by

[15] This construction embeds the fan $\mathcal{N}_{\mathsf{M}_{\boldsymbol{c}}(\mathsf{P})}$ directly into the hyperplane $\boldsymbol{c}^\perp$, instead of embedding it in $\mathbb{R}^{\dim(\mathsf{P})}$.

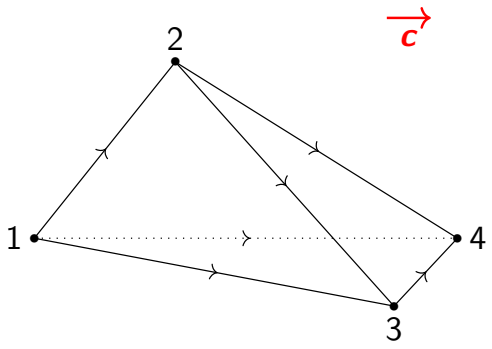

Figure 56: Animated construction of the normal fan of the monotone path polytope of the 3-dimensional simplex. For each $\boldsymbol{\omega} \in \mathbb{R}^3$ orthogonal to $\boldsymbol{c}$, we project Δ_3 onto the plane $(\boldsymbol{c}, \boldsymbol{\omega})$ (Left), and record the corresponding coherent monotone path (Right). note that, contrarily to Figure 26, we only score the upper path of each projection of the tetrahedron, not the full arborescence. *(Animated figures obviously do not display on paper, and some PDF readers do not support the format: it is advised to use Adobe Acrobat Reader. If no solution is suitable, the animation can be found on my website or asked by email.)*

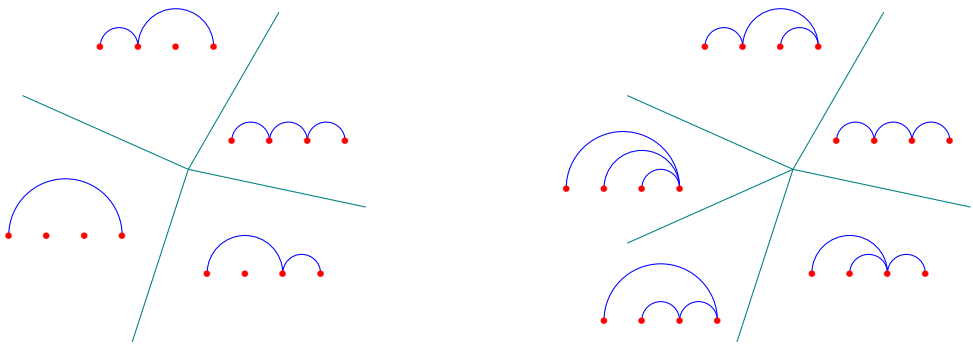

Fan of $\mathsf{M}_{\boldsymbol{c}}(\Delta_3)$ Fan of $\Pi(\Delta_3, \boldsymbol{c})$

Figure 57: The normal fan of $\mathsf{M}_{\boldsymbol{c}}(\mathsf{P})$ coarsens the one of $\Pi(\mathsf{P}, \boldsymbol{c})$. Here is drawn the example for the tetrahedron $\mathsf{P} = \Delta_3$.

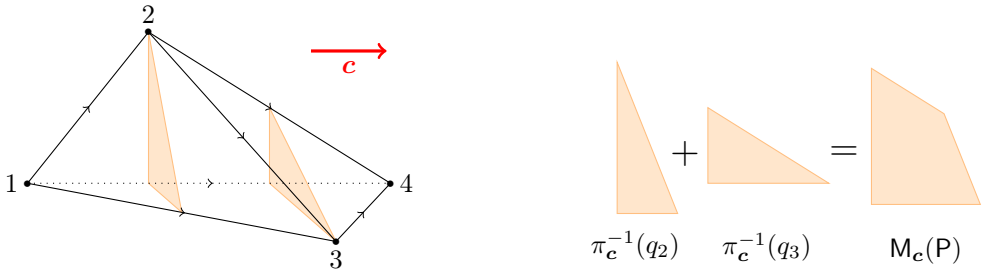

Figure 58: The construction of $\mathsf{M}_{\boldsymbol{c}}(\mathsf{P})$ as a sum of sections for the tetrahedron $\mathsf{P} = \Delta_3$. Each section is orthogonal to $\boldsymbol{c}$ and contains a vertex (except for $\boldsymbol{v}_{\min}$ and $\boldsymbol{v}_{\text{opt}}$).

induction that $\Gamma_{k+1} = \sum_{i=1}^{k+1} \gamma_i$ is normally equivalent to $Z_k = \sum_{i=1}^{k} \zeta_i(\frac{1}{2})$. As Z_{n-1} is normally equivalent to $M_{\boldsymbol{c}}(P)$ by Theorem 4.7, this will prove the theorem.

All $\zeta_i(\lambda)$ are normally equivalent for $\lambda \in]0,1[$, and γ_{i+1} is a deformation of $\zeta_i(\lambda)$. Thus Γ_n is a deformation of Z_n. Furthermore, suppose a face f of $\zeta_i(\lambda)$ does not appear in the deformation γ_{i+1} and let F be the corresponding intersected face in P. Then $\boldsymbol{v}_{i+1}$ is the last vertex of F, and there exists a vertex $\boldsymbol{v}_j$ with $j \leq i$ in F: then in γ_j, the face f appears.

This fact has two consequences. On one side, Γ_2 is normally equivalent to Z_1 as the only possible face with last vertex $\boldsymbol{v}_2$ is the edge $[\boldsymbol{v}_1, \boldsymbol{v}_2]$ which section is a point. On the other side, suppose Γ_{k+1} is normally equivalent to Z_k, and consider a face in $Z_k + \zeta_{k+1}$. This face either appears in one of the γ_i for $i \leq k+1$, or in γ_{k+2}. As the normal fan of a Minkowski sum is the common refinement of the normal fans of the summands, the polytopes Γ_{k+2} and Z_{k+1} are normally equivalent. □

The rest of this section is devoted to the monotone path polytopes of hypersimplices, and especially hypersimplices for $k = 2$. Before presenting new results on this subject, we shortly recall two former results from Billera and Sturmfels [BS92, end of Section 5].

Theorem 4.16 ([BS92]). *For any simplex Δ on $n+1$ vertices, and any generic direction $\boldsymbol{c}$, the monotone path polytope $M_{\boldsymbol{c}}(\Delta)$ is (isomorphic to) a cube of dimension $n-1$.*

Theorem 4.17 ([BS92]). *For the standard cube $\square_d = [0,1]^n$ of dimension n, and the direction $\boldsymbol{c} = (1, \dots, 1)$, the monotone path polytope $M_{\boldsymbol{c}}(\square_d)$ is (a dilation of) the permutahedron Π_n of dimension $n-1$.*

These two results motivate the study of the monotone path polytopes of hypersimplices. Indeed, hypersimplices are a generalization of simplices, and arise as sections of the standard cube.

Definition 4.18. For $n \geq 2$, $k \in [n]$, the *(n,k)-hypersimplex* is $\Delta(n,k) = \left\{\boldsymbol{x} \in [0,1]^n \ ; \ \sum_i x_i = k\right\}$. It is the section of the standard cube $\square_d = [0,1]^n$ by the hyperplane $\{\boldsymbol{x} \in \mathbb{R}^n \ ; \ \langle \boldsymbol{x}, (1, \dots, 1)\rangle = k\}$.

The vertices of $\Delta(n,k)$ are exactly its $(0,1)$-coordinate elements: the $(0,1)$-vectors with k ones and $n-k$ zeros. We denote the *support* of a vertex $\boldsymbol{v} \in V(\Delta(n,k))$ by $s(\boldsymbol{v}) := \{i \ ; \ v_i = 1\}$. Two vertices $\boldsymbol{u}, \boldsymbol{v} \in V(\Delta(n,k))$ share an edge when $|s(\boldsymbol{u}) \cap s(\boldsymbol{v})| = k-1$, *i.e.* to obtain $\boldsymbol{v}$ from $\boldsymbol{u}$, flip a zero to a one and a one to a zero.

Note that the hypersimplices $\Delta(n,1)$ and $\Delta(n,n-1)$ are simplices: in this sense, hypersimplices are a generalization of simplices.

We consider the linear problem $(\Delta(n,k), \boldsymbol{c})$ where $\boldsymbol{c} \in \mathbb{R}^n$ is generic with respect to $\Delta(n,k)$. The vector $\boldsymbol{c} \in \mathbb{R}^n$ will be fixed for the rest of this analysis of monotone path polytopes of the hypersimplices. See Figure 59(Left) for an example. We denote $M(n,k) := M_{\boldsymbol{c}}(\Delta(n,k))$ to ease notations. Such a $\boldsymbol{c}$ is generic for the hypersimplex when $c_i \neq c_j$ for all $i \neq j$, as each edge has direction $\boldsymbol{e}_i - \boldsymbol{e}_j$. Without lost of generality, as the hypersimplex is invariant under reordering coordinates, we suppose $c_1 < c_2 < \cdots < c_n$. Note however that there can exist $\boldsymbol{v}, \boldsymbol{w} \in V(\Delta(n,k))$ with $\langle \boldsymbol{v}, \boldsymbol{c}\rangle = \langle \boldsymbol{w}, \boldsymbol{c}\rangle$ (when $\boldsymbol{v}$ and $\boldsymbol{w}$ are not adjacent vertices). When drawing, we will take $\boldsymbol{c} = (1, 2, \dots, n)$.

We denote $\boldsymbol{v}_{\min} = (1, \dots, 1, 0, \dots, 0) \in V(\Delta(n,k))$ the vertex of $\Delta(n,k)$ minimizing $\langle \boldsymbol{v}, \boldsymbol{c}\rangle$ for $\boldsymbol{v} \in V(\Delta(n,k))$, and $\boldsymbol{v}_{\max} = (0, \dots, 0, 1, \dots, 1) \in V(\Delta(n,k))$ the vertex of $\Delta(n,k)$ maximizing $\langle \boldsymbol{v}, \boldsymbol{c}\rangle$ for $\boldsymbol{v} \in V(\Delta(n,k))$. We now interpret the conditions for being a coherent monotone path on a polytope for the case of the hypersimplex $\Delta(n,k)$.

Definition 4.19. A *monotone path of vertices* $P = (\boldsymbol{v}_1, ..., \boldsymbol{v}_r)$ on $\Delta(n,k)$ is an ordered list of vertices of $\Delta(n,k)$ such that $\boldsymbol{v}_1 = \boldsymbol{v}_{\min}$, $\boldsymbol{v}_r = \boldsymbol{v}_{\max}$ and for all $i \in [r-1]$, $(\boldsymbol{v}_i, \boldsymbol{v}_{i+1})$ is an *improving edge* of $\Delta(n,k)$ for $\boldsymbol{c}$, *i.e.* an edge of $\Delta(n,k)$ with $\langle \boldsymbol{v}_i, \boldsymbol{c}\rangle < \langle \boldsymbol{v}_{i+1}, \boldsymbol{c}\rangle$. The *length* of P is r.

For all $i \in [1, r-1]$, the vertices $\boldsymbol{v}_i$ and $\boldsymbol{v}_{i+1}$ form an edge of $\Delta(n,k)$. Thus, instead of considering the path P as a list of vertices, we emphasize what changes and what remains between $\boldsymbol{v}_i$ and $\boldsymbol{v}_{i+1}$ by storing the enhanced steps of P. The *i-th enhanced step* of P is denoted $x \xrightarrow{Z} y$ with:

- Z the common support, *i.e.* $Z = \mathrm{s}(\boldsymbol{v}_i) \cap \mathrm{s}(\boldsymbol{v}_{i+1})$.
- x the only index in the support of $\boldsymbol{v}_i$ that is not in the support of $\boldsymbol{v}_{i+1}$, *i.e.* $\{x\} = \mathrm{s}(\boldsymbol{v}_i) \smallsetminus \mathrm{s}(\boldsymbol{v}_{i+1})$.
- y the only index in the support of $\boldsymbol{v}_{i+1}$ that is not in the support of $\boldsymbol{v}_i$, *i.e.* $\{y\} = \mathrm{s}(\boldsymbol{v}_{i+1}) \smallsetminus \mathrm{s}(\boldsymbol{v}_i)$.

The list of enhanced steps of P is denoted $\mathcal{S}(P)$. The application $P \mapsto \mathcal{S}(P)$ is obviously injective. When $a \xrightarrow{C} b$ is the i-th enhanced step, and $x \xrightarrow{Z} y$ the j-th one, with $i < j$, we denote $a \xrightarrow{C} b \prec x \xrightarrow{Z} y$ and say that $a \xrightarrow{C} b$ *precedes* $x \xrightarrow{Z} y$.

A monotone path is said *coherent* when it corresponds to a vertex of $\mathsf{M}(n,k)$.

Proposition 4.20. *For $\boldsymbol{\omega} \in \mathbb{R}^n$, let $\pi^{\boldsymbol{\omega}} : \mathbb{R}^n \to \mathbb{R}^2$ be the projection $\pi^{\boldsymbol{\omega}}(\boldsymbol{x}) = \big(\langle \boldsymbol{x}, \boldsymbol{c}\rangle\,,\ \langle \boldsymbol{x}, \boldsymbol{\omega}\rangle\big)$. In particular, for a vertex $\boldsymbol{v} \in V(\Delta(n,k))$, then $\pi^{\boldsymbol{\omega}}(\boldsymbol{v}) = \big(\sum_{i\in s(\boldsymbol{v})} c_i,\ \sum_{i\in s(\boldsymbol{v})} \omega_i\big)$.*

A monotone path of vertices $P = (\boldsymbol{v}_1, \dots \boldsymbol{v}_r)$ is coherent if and only if there exists $\boldsymbol{\omega} \in \mathbb{R}^n$ such that for all $i \in [1, r-1]$:

$$\forall J \in \binom{[n]}{k}, \qquad \sum_{j\in J} c_j > \sum_{p\in s(\boldsymbol{v}_i)} c_p \implies \tau_{\boldsymbol{\omega}}\big(s(\boldsymbol{v}_i), J\big) < \tau_{\boldsymbol{\omega}}\big(s(\boldsymbol{v}_i), s(\boldsymbol{v}_{i+1})\big)$$

where $\tau_{\boldsymbol{\omega}}(I,J) = \frac{\sum_{j\in J}\omega_j - \sum_{i\in I}\omega_i}{\sum_{j\in J} c_j - \sum_{i\in I} c_i}$ is the slope between the point $\big(\sum_{i\in I} c_i,\ \sum_{i\in I}\omega_i\big)$ and the point $\big(\sum_{i\in J} c_j,\ \sum_{j\in J}\omega_j\big)$, see Figure 61(Top). We say that such $\boldsymbol{\omega}$ captures P.

Proof. By Definition 4.4, a monotone path of vertices P is coherent if and only if there exists $\boldsymbol{\omega} \in \mathbb{R}^n$ such that the upper path of the polygon $\pi^{\boldsymbol{\omega}}(\Delta(n,k))$ is precisely $\pi^{\boldsymbol{\omega}}(P) := \big(\pi^{\boldsymbol{\omega}}(\boldsymbol{v})\big)_{\boldsymbol{v}\in P}$ (remember we take the upper faces instead of the lower faces by convention in the section).

If $\boldsymbol{v} \in V(\Delta(n,k))$ is in the upper path of $\pi^{\boldsymbol{\omega}}(\Delta(n,k))$, then the next vertex in the upper path is the improving neighbor $\boldsymbol{v}'$ of $\boldsymbol{v}$ that maximizes the slope $\frac{\langle \boldsymbol{v}'-\boldsymbol{v}, \boldsymbol{\omega}\rangle}{\langle \boldsymbol{v}'-\boldsymbol{v}, \boldsymbol{c}\rangle}$. As $\boldsymbol{c}$ is generic for $\Delta(n,k)$, the vertex $\boldsymbol{u} \in V(\Delta(n,k))$ maximizing this slope is necessarily an improving neighbor of $\boldsymbol{v}$, as the pre-image of edge $\big[\pi^{\boldsymbol{\omega}}(\boldsymbol{v}), \pi^{\boldsymbol{\omega}}(\boldsymbol{u})\big]$ in the polygon $\pi^{\boldsymbol{\omega}}(\Delta(n,k))$ is an (improving) edge in $\Delta(n,k)$. Consequently, the condition stated in the proposition is both necessary and sufficient. □

Example 4.21. The hypersimplex $\Delta(3,2)$ is a triangle, that is to say a simplex of dimension 2. By Billera–Sturmfels' Theorem 4.16, for any $\boldsymbol{c} \in \mathbb{R}^3$, its monotone path polytope is a cube of dimension 1: it has 2 vertices, one corresponding to the path of length 3 and the other to the path of length 2.

Example 4.22. On the hypersimplex $\Delta(4,2)$, for $\boldsymbol{c} = (1,2,3,4)$ there are 8 coherent monotone paths, and 2 non-coherent monotone paths. The 8 coherent monotone paths correspond to the vertices of the octagon $\mathsf{M}(4,2)$ depicted on Figure 59(Right). There are 4 coherent monotone paths of length 3, and 4 coherent monotone paths of length 4. On the other side, the 2 non-coherent monotone paths are of length 5: $(1100, 1010, \mathbf{0110}, 0101, 0011)$ and $(1100, 1010, \mathbf{1001}, 0101, 0011)$, in bold are the vertices that differ between the two paths.

With a quick jotting, one can prove that for all $\boldsymbol{c} \in \mathbb{R}^4$, the same holds: for all $\boldsymbol{c} \in \mathbb{R}^4$, the coherent monotone paths are exactly the same. This can also be retrieved from [BL21, Theorem 3.2] as $\Delta(4,2)$ is the cross-polytope of dimension 3.

Example 4.23. To be able to draw the monotone path polytope $\mathsf{M}(n,k)$ of the hypersimplex $\Delta(n,k)$, we need that $\dim \Delta(n,k) \le 4$, so that $\dim \mathsf{M}(n,k) \le 3$. This implies $n \le 5$. Moreover, remember that $\Delta(n,k)$ is linearly isomorphic to $\Delta(n, n-k)$. For $n = 3$, Example 4.21 deals with $k = 2$ (and thus $k = 1$ by symmetry). For $n = 4$, Example 4.22 deals with $k = 2$, while $\Delta(4,k)$ with $k = 1$ and $k = 3$ are simplices and their monotone path polytopes are squares. For $n = 5$, $\Delta(5,k)$ with $k = 1$ and $k = 4$ are simplices and their monotone path polytopes are cubes, while $k = 2$ and $k = 3$ are equivalent and their monotone path polytope is depicted in Figure 60: it has 33 vertices, 52 edges, and 21 faces (5 octagons and 16 squares).

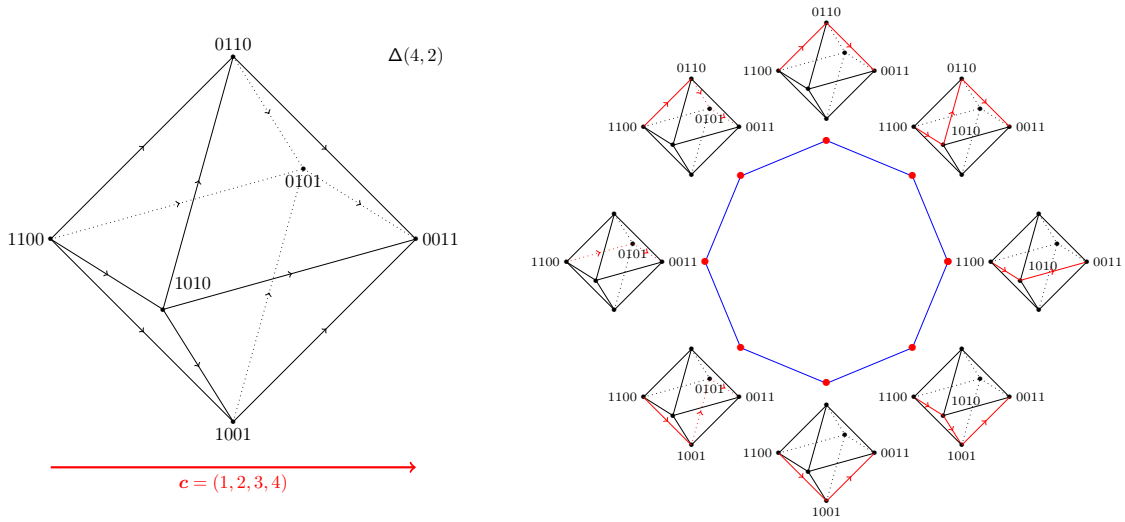

Figure 59: (Left) The $(4,2)$-hypersimplex lives in the hyperplane $\{\boldsymbol{x}\ ;\ \sum_{i=1}^{4} x_i = 2\}$ inside $\mathbb{R}^4$. (Right) The monotone path polytope $\mathsf{M}(4,2)$ is an octagon, each vertex of which is labelled by the corresponding monotone path (drawn on $\Delta(4,2)$).

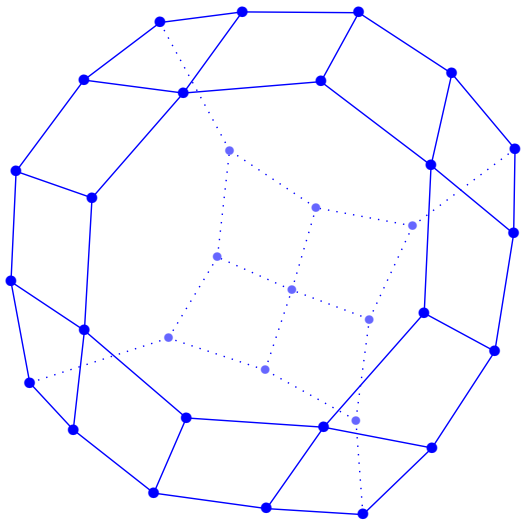

Figure 60: The monotone path polytope $\mathsf{M}(5,2)$ of the hypersimplex $\Delta(5,2)$. This hypersimplex is linearly equivalent to $\Delta(5,3)$. As $\Delta(5,2)$ has 5 facets linearly equivalent to $\Delta(4,2)$, its monotone path polytope $\mathsf{M}(5,2)$ has 5 facets which are isomorphic to $\mathsf{M}(4,2)$ *i.e.* octagons.

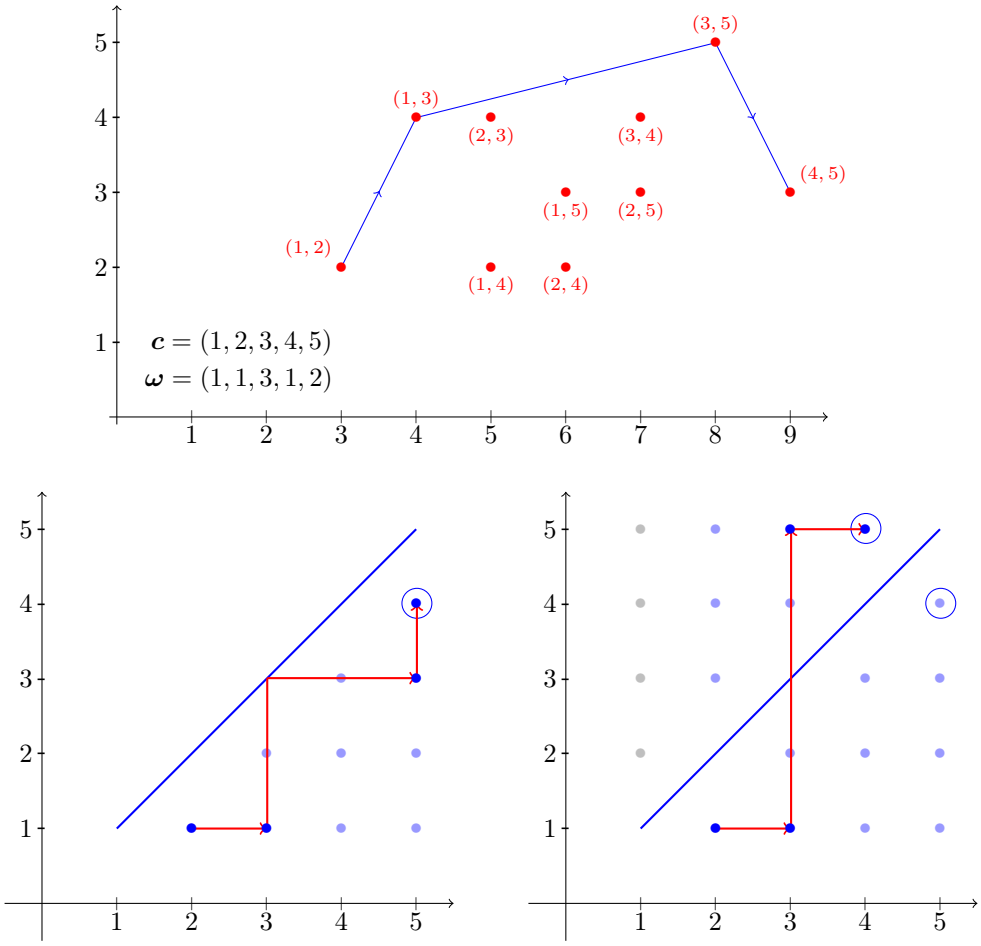

Figure 61: (Top) For the given $\boldsymbol{c}$ and $\boldsymbol{\omega}$, the hypersimplex $\Delta(5,2)$ is projected the 10 points drawn, where each vertex of $\Delta(5,2)$ is indicated by its support. The coherent path P captured is drawn in blue. (Bottom) P corresponds to the diagonal-avoiding path depicted on the right, while associating P to lattice points (x,y) with $x < y$ give the bottom left figure.

4.2.2 A necessary criterion for coherent paths on $\Delta(n,k)$

Even if Proposition 4.20 gives an efficient criterion for determining which monotone path a given $\boldsymbol{\omega}$ does capture, the question we want to answer is the converse one: how to characterize the coherent paths on the hypersimplex? In this section, we present a necessary criterion for a monotone path to be coherent, and in the next one, we prove this criterion is sufficient in the case of the $(n,2)$-hypersimplices (but not sufficient in general).

Theorem 4.24. *If path P is coherent, then for all couples of enhanced steps $i \xrightarrow{A} j \prec x \xrightarrow{Z} y$ with $x < j$, one has $j \in Z$ or $x \in A$.*

Before proving this criterion, we will introduce a simple but powerful lemma. In essence, this lemma states that there exist only two kinds of triangles in the plane: upwards pointing ones $\triangle$ and downwards pointing ones ∇. This lemma is equivalent to Lemma 3.5, but we give it here again to make the section self contained.

Lemma 4.25. *For three points in the plane (x_1,y_1), (x_2,y_2) and (x_3,y_3) with $x_1 < x_2 < x_3$, denote the slopes $\tau(1,2) = \frac{y_2-y_1}{x_2-x_1}$, $\tau(2,3) = \frac{y_3-y_2}{x_3-x_2}$ and $\tau(1,3) = \frac{y_3-y_1}{x_3-x_1}$. Then $\tau(1,3)$ is a convex combination of the slopes $\tau(1,2)$ and $\tau(2,3)$. In particular, if $\tau(1,2) < \tau(1,3)$, then $\tau(1,3) < \tau(2,3)$ (and conversely if $\tau(1,2) > \tau(1,3)$, then $\tau(1,3) > \tau(2,3)$).*

Proof. One has the convex combination: $\tau(1,3) = \frac{x_2-x_1}{x_3-x_1}\tau(1,2) + \frac{x_3-x_2}{x_3-x_1}\tau(2,3)$ □

Proof of Theorem 4.24. Suppose $i \xrightarrow{A} j \prec x \xrightarrow{Z} y \in \mathcal{S}(P)$ with $x < j$ (so $c_x < c_j$), $j \notin Z$ and $x \notin A$. Fix $\boldsymbol{\omega} \in \mathbb{R}^n$ that captures P. Then consider $\boldsymbol{v}_1$, $\boldsymbol{v}_2$ with $\mathrm{s}(\boldsymbol{v}_1) = A \cup \{i\}$, $\mathrm{s}(\boldsymbol{v}_2) = A \cup \{j\}$, and $\boldsymbol{v}_3$, $\boldsymbol{v}_4$ with $\mathrm{s}(\boldsymbol{v}_3) = Z \cup \{x\}$, $\mathrm{s}(\boldsymbol{v}_4) = Z \cup \{y\}$, see Figure 62. These are 4 vertices of $\Delta(n,k)$ in the path P. Abusing notation, we write $\tau_{\boldsymbol{\omega}}(\boldsymbol{u},\boldsymbol{v})$ instead of $\tau_{\boldsymbol{\omega}}\big(\mathrm{s}(\boldsymbol{u}),\mathrm{s}(\boldsymbol{v})\big)$ when the context is clear.

As $x \notin A$, there exists $\boldsymbol{u}_1 \in V(\Delta(n,k))$ with $\mathrm{s}(\boldsymbol{u}_1) = A \cup \{x\}$, thus $\boldsymbol{v}_2$ is an improving neighbor of $\boldsymbol{u}_1$. As $j \notin Z$, there exists $\boldsymbol{u}_2 \in V(\Delta(n,k))$ with $\mathrm{s}(\boldsymbol{u}_2) = Z \cup \{j\}$, thus $\boldsymbol{u}_2$ is an improving neighbor of $\boldsymbol{v}_3$. First observe that, $\tau_{\boldsymbol{\omega}}\big(\boldsymbol{v}_1,\boldsymbol{u}_1\big) < \tau_{\boldsymbol{\omega}}\big(\boldsymbol{v}_1,\boldsymbol{v}_2\big)$ by Proposition 4.20, thus $\tau_{\boldsymbol{\omega}}\big(\boldsymbol{u}_1,\boldsymbol{v}_2\big) > \tau_{\boldsymbol{\omega}}\big(\boldsymbol{v}_1,\boldsymbol{v}_2\big)$ by Lemma 4.25 applied in the triangle $\pi_{\boldsymbol{\omega}}(\boldsymbol{v}_1)$, $\pi_{\boldsymbol{\omega}}(\boldsymbol{v}_2)$, $\pi_{\boldsymbol{\omega}}(\boldsymbol{u}_1)$. Moreover, $\tau_{\boldsymbol{\omega}}\big(\boldsymbol{v}_3,\boldsymbol{u}_2\big) < \tau_{\boldsymbol{\omega}}\big(\boldsymbol{v}_3,\boldsymbol{v}_4\big)$ by Proposition 4.20. As $\pi_{\boldsymbol{\omega}}(P)$ is convex: $\tau_{\boldsymbol{\omega}}\big(\boldsymbol{v}_1,\boldsymbol{v}_2\big) > \tau_{\boldsymbol{\omega}}\big(\boldsymbol{v}_3,\boldsymbol{v}_4\big)$ because the second step comes later in the path. But then: $\tau_{\boldsymbol{\omega}}\big(\boldsymbol{u}_1,\boldsymbol{v}_2\big) < \tau_{\boldsymbol{\omega}}\big(\boldsymbol{v}_3,\boldsymbol{u}_2\big)$, while in the meantime: $\tau_{\boldsymbol{\omega}}\big(\boldsymbol{u}_1,\boldsymbol{v}_2\big) = \frac{\omega_j-\omega_x}{c_j-c_x} = \tau_{\boldsymbol{\omega}}\big(\boldsymbol{v}_3,\boldsymbol{u}_2\big)$. This contradiction proves the theorem. □

4.2.3 Sufficiency of this criterion in the case $\Delta(n,2)$

We are going to prove that for $\Delta(n,2)$, the criterion of Theorem 4.24 is actually sufficient. To this end, we want to associate monotone paths on $\Delta(n,k)$ with some lattice paths on the integer grid $[n]^k$. A first idea to do so would be to associate to each vertex $\boldsymbol{v}_i$ in the path $P = (\boldsymbol{v}_1,\dots\boldsymbol{v}_r)$ a point $\boldsymbol{\ell}_i = (\ell_{i,1},\dots,\ell_{i,k}) \in [n]^k$ satisfying $\{\ell_{i,1},\dots,\ell_{i,k}\} = \mathrm{s}(\boldsymbol{v}_i)$. This leaves $k!$ possible choices for $\boldsymbol{\ell}_i$. Even though a *natural* choice would be to impose $\ell_{i,1} < \cdots < \ell_{i,k}$, we will prefer another one. Indeed, as $\boldsymbol{v}_i$ and $\boldsymbol{v}_{i+1}$ form an edge of $\Delta(n,k)$, there is only one index differing between $\mathrm{s}(\boldsymbol{v}_i)$ and $\mathrm{s}(\boldsymbol{v}_{i+1})$, so we will impose that $\boldsymbol{\ell}_i$ and $\boldsymbol{\ell}_{i+1}$ differ at only one coordinate.

Although this idea allows us to embed our problem into the realm of lattice paths, it has for drawback to associate $k!$ different lattice points to a same vertex, see Figure 61(Bottom).

Definition 4.26. A *diagonal-avoiding lattice path* $\mathcal{L} = (\boldsymbol{\ell}_1,\dots,\boldsymbol{\ell}_r)$ of *size* n and *dimension* k is an ordered list of points $\boldsymbol{\ell}_i \in [n]^k$ such that:

- $\boldsymbol{\ell}_1 = (k, k-1, \dots, 1)$;
- $\boldsymbol{\ell}_r = (\ell_{r,1},\dots,\ell_{r,k})$ with $\{\ell_{r,1},\dots,\ell_{r,k}\} = \{n-k+1,\dots,n\}$;
- for all $i \in [r]$, $\ell_{i,p} \neq \ell_{i,q}$ for all $p,q \in [k]$ with $p \neq q$;

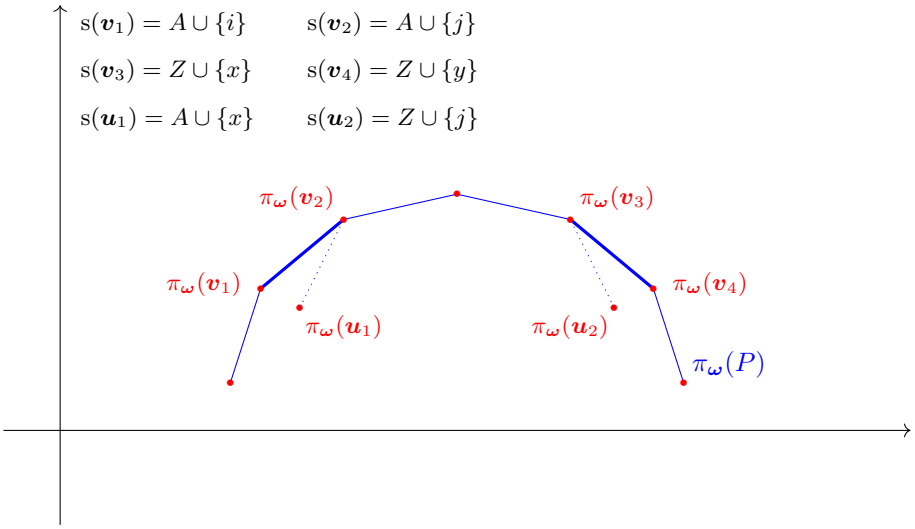

Figure 62: Dotted slopes shall be both equal to $\frac{\omega_j - \omega_x}{c_j - c_x}$: this is impossible if $\pi_{\boldsymbol{\omega}}(\boldsymbol{u}_1)$ and $\pi_{\boldsymbol{\omega}}(\boldsymbol{u}_2)$ are below $\pi_{\boldsymbol{\omega}}(P)$, thus either $\boldsymbol{u}_1$ or $\boldsymbol{u}_2$ is not a vertex of $\Delta(n,k)$ (*i.e.* $|s(\boldsymbol{u}_1)| \leq k-1$ or $|s(\boldsymbol{u}_2)| \leq k-1$).

- for all $i \in [r-1]$, there exists a $p \in [k]$ such that $\ell_{i,p} < \ell_{i+1,p}$, and $\ell_{i,q} = \ell_{i+1,q}$ for all $q \neq p$. The *i-th enhanced step* of $\mathcal{L}$ is denoted $\ell_{i,p} \xrightarrow{Z} \ell_{i+1,p}$ with $Z = \{\ell_{i,q} \ ; \ q \neq p\}$.

The ordered list of enhanced steps of $\mathcal{L}$ is denoted $\mathcal{S}(\mathcal{L})$. The *length* of $\mathcal{L}$ is r.

To a path $P = (\boldsymbol{v}_1, \dots \boldsymbol{v}_r)$ on $\Delta(n,k)$, one can associate a diagonal-avoiding lattice path $\mathscr{L}(P) = (\boldsymbol{\ell}_1, \dots, \boldsymbol{\ell}_r)$ of size n and dimension k defined by $\mathcal{S}(\mathscr{L}(P)) = \mathcal{S}(P)$, see Figure 63.

Proposition 4.27. *The map $P \mapsto \mathscr{L}(P)$ is a bijection from monotone paths on $\Delta(n,k)$ to diagonal-avoiding lattice paths of size n and dimension k.*

Proof. Fix a monotone path P on $\Delta(n,k)$. Starting at $\boldsymbol{\ell}_1 = (k, k-1, \dots, 1)$, the lattice path $\mathscr{L}(P) = (\boldsymbol{\ell}_1, \dots, \boldsymbol{\ell}_i, \dots, \boldsymbol{\ell}_r)$ can be defined by induction on i. Indeed, denote by $\mathscr{L}(P)_{\leq i} = (\boldsymbol{\ell}_1, \dots, \boldsymbol{\ell}_i)$, and suppose that for a fixed i: $\{\ell_{j,1}, \dots, \ell_{j,k}\} = s(\boldsymbol{v}_j)$ for all $j \leq i$, and the enhanced steps of $\mathscr{L}(P)_{\leq i}$ are the $(i-1)$ first enhanced steps of P. Consider the i-th enhanced step of P, say $x \xrightarrow{Z} y$. As $\{\ell_{i,1}, \dots, \ell_{i,k}\} = s(\boldsymbol{v}_j)$, there exists $p \in [k]$ such that $\ell_{i,p} = x$, and $\{\ell_{i,1}, \dots, \ell_{i,k}\} \smallsetminus \{\ell_{i,p}\} = Z$. By setting $\boldsymbol{\ell}_{i+1}$ with $\ell_{i+1,q} = \ell_{i,q}$ for $q \neq p$, and $\ell_{i+1,p} = y$, we construct $\mathscr{L}(P)_{\leq i+1}$ that fulfills the induction hypothesis. Hence, we can define $\mathscr{L}(P)$ such that $\mathcal{S}(\mathscr{L}(P)) = \mathcal{S}(P)$. By induction, $\mathscr{L}(P)$ satisfies that $\{\ell_{i,1}, \dots, \ell_{i,k}\} = s(\boldsymbol{v}_i)$. Moreover, as $|s(\boldsymbol{v}_i)| = k$, we know that $\ell_{i,p} \neq \ell_{i,q}$ for all $p \neq q$. Consequently, as $s(\boldsymbol{v}_i)$ and $s(\boldsymbol{v}_{i+1})$ differ by only one element, $\mathscr{L}(P)$ is a diagonal-avoiding path.

As $P \mapsto \mathcal{S}(P)$ is injective, it is immediate that $P \mapsto \mathscr{L}(P)$ is also injective.

Finally, for all diagonal-avoiding paths $\mathcal{L} = (\boldsymbol{\ell}_1, \dots, \boldsymbol{\ell}_r)$, one can construct by induction an ordered list of vertices $P_{\mathcal{L}} = (\boldsymbol{v}_1, \dots, \boldsymbol{v}_r)$ by taking $\boldsymbol{v}_i = \sum_{j \in \boldsymbol{\ell}_i} \boldsymbol{e}_j$. Such a path $P_{\mathcal{L}}$ is a monotone path on $\Delta(n,k)$ thanks to the properties of diagonal-avoiding paths. Moreover, as $\mathcal{S}(P_{\mathcal{L}}) = \mathcal{S}(\mathcal{L})$, the map $\mathcal{L} \mapsto P_{\mathcal{L}}$ is the reciprocal of $P \mapsto \mathscr{L}(P)$. □

Remark 4.28. It is straightforward to see that the length of P, *i.e.* the number of vertices contained in P, equals the length of $\mathscr{L}(P)$, *i.e.* the number of lattice points contained in $\mathscr{L}(P)$.

Example 4.29. For size $n = 3$, there are 2 diagonal-avoiding paths, one of length 1 and one of length 2. As seen in Example 4.21, all of them are images (by $\mathscr{L}$) of coherent paths on the simplex $\Delta(3,2)$.

$$\mathcal{S}(P) = \left(2 \xrightarrow{1} 4,\ \ 1 \xrightarrow{4} 5,\ \ 4 \xrightarrow{5} 6,\ \ 6 \xrightarrow{5} 7,\ \ 7 \xrightarrow{5} 8,\ \ 5 \xrightarrow{8} 7\right)$$

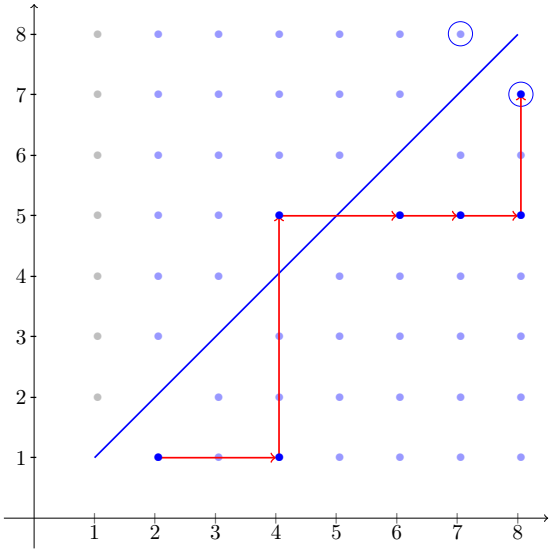

Figure 63: The lattice path associated to the ordered list of enhanced steps given on Top. It has size 8, dimension 2 and length 6.

For size $n = 4$, there are 10 diagonal-avoiding paths, see Figure 64. As seen in Example 4.22, 8 of them are images (by $\mathscr{L}$) of coherent paths on $\Delta(4, 2)$, while 2 come from monotone but not coherent paths on $\Delta(4, 2)$.

To ease notation, for an enhanced step of a path P on $\Delta(n, 2)$ or enhanced steps of diagonal-avoiding lattice paths of dimension 2, we will write $i \xrightarrow{a} j$ instead of $i \xrightarrow{\{a\}} j$. We will now study diagonal-avoiding paths of dimension 2. In particular, we will show that coherent monotone paths on $\Delta(n, 2)$ are associated with a certain family of diagonal-avoiding lattice paths, and that this family respects an induction process (which is cumbersome but powerful). To describe this induction process for our family, we need the notion of *restriction* of diagonal-avoiding lattice paths, which consists in shrinking the lattice grid $[n]^2$: suppose given a diagonal-avoiding lattice path on $[n+1]^2$, then erase the points of $[n+1]^2 \setminus [n]^2$; the path obtained on $[n]^2$ will probably not end at the right spot, but you can complete it to mimic the path you started with. The following definition formalizes this idea.

Definition 4.30. The *restriction* of a diagonal-avoiding lattice path $\mathcal{L} = (\boldsymbol{\ell}_1, \ldots, \boldsymbol{\ell}_r)$ of size $n + 1$ and dimension 2 is the diagonal-avoiding lattice path $\mathcal{L}' = (\boldsymbol{\ell}'_1, \ldots, \boldsymbol{\ell}'_s)$ of size n and dimension 2 defined by:

1. First, for all $i \in [r]$ define $\ell'_{i,p} = \begin{cases} \ell_{i,p} & \text{if } \ell_{i,p} \neq n+1 \\ n & \text{else} \end{cases}$ (for $p \in \{1, 2\}$) with $s = r$,
2. Next, as $\boldsymbol{\ell}'_r = (n, n)$: if $\boldsymbol{\ell}'_{r-1} = (x, n)$ then set $\boldsymbol{\ell}'_r = (n - 1, n)$, whereas if $\boldsymbol{\ell}'_{r-1} = (n, x)$ then set $\boldsymbol{\ell}'_r = (n, n - 1)$;
3. Finally, if $\boldsymbol{\ell}'_i = \boldsymbol{\ell}'_{i+1}$, then discard $\boldsymbol{\ell}'_{i+1}$ (and keep discarding until no doubles remain).

Even though this definition seems convoluted, it has a very straightforward illustration, see Figure 65: as explained before, draw the path $\mathcal{L}$ on the $(n + 1) \times (n + 1)$ grid, then $\mathcal{L}'$ is obtained by first restricting $\mathcal{L}$ to the $n \times n$ grid, then mimicking the steps $i \xrightarrow{n+1} j$ of $\mathcal{L}$ by introducing the steps $i \xrightarrow{n} j$ in $\mathcal{L}'$ (and slightly modifying $\mathcal{L}'$ to make it diagonal-avoiding).

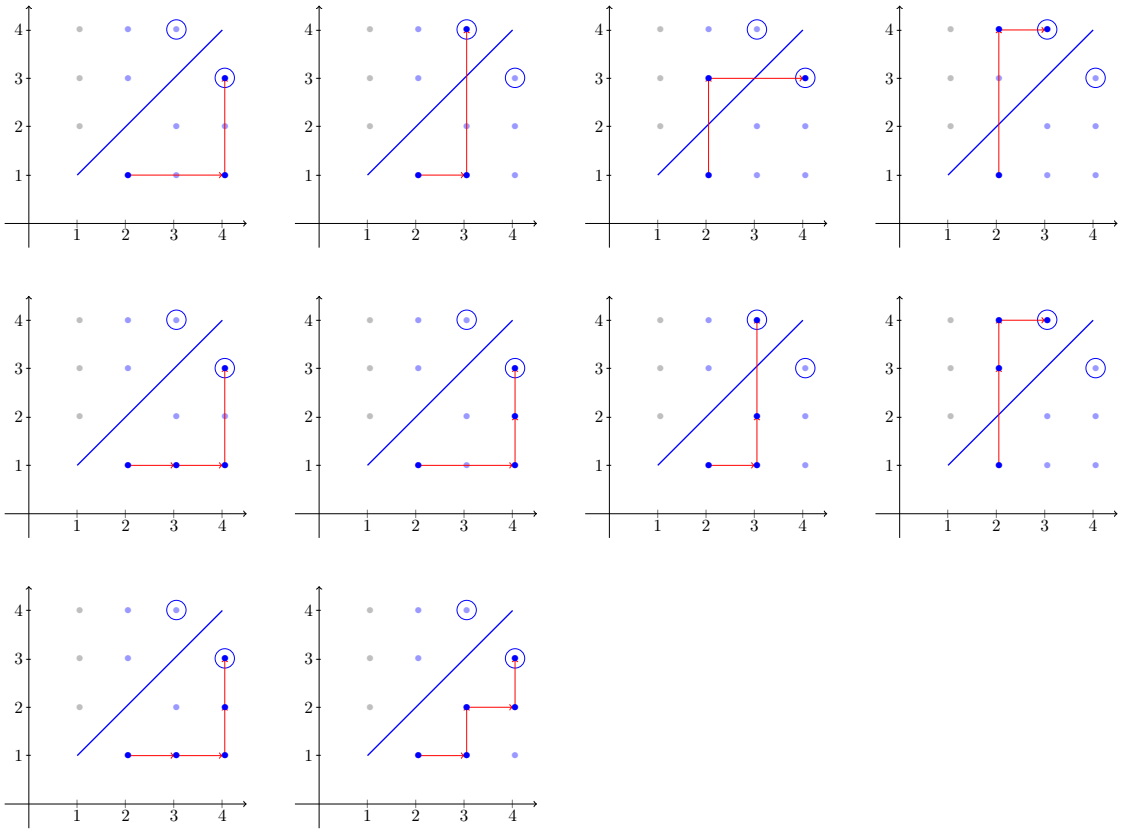

Figure 64: All 10 diagonal-avoiding lattice paths of size 4 and dimension 2, sorted by size.

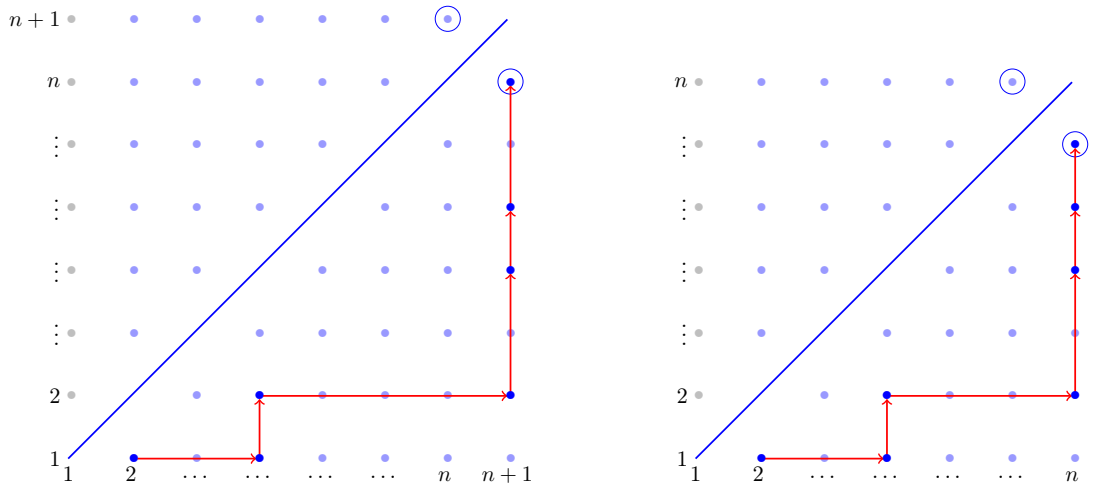

Figure 65: The restriction of $\mathcal{L}$ to $\mathcal{L}'$ restrict its enhanced steps from $\mathcal{S}(\mathcal{L}) = \big(2 \xrightarrow{1} 4,\ 1 \xrightarrow{4} 2,\ 4 \xrightarrow{2} n+1,\ 2 \xrightarrow{n+1} 4,\ 4 \xrightarrow{n+1} 5,\ 5 \xrightarrow{n+1} n\big)$ to $\mathcal{S}(\mathcal{L}') = \big(2 \xrightarrow{1} 4,\ 1 \xrightarrow{4} 2,\ 4 \xrightarrow{2} n,\ 2 \xrightarrow{n} 4,\ 4 \xrightarrow{n} 5,\ 5 \xrightarrow{n} n-1\big)$.

We can now introduce the main object of this section:

Definition 4.31. A diagonal-avoiding lattice path $\mathcal{L}$ of dimension 2 is said to be a *coherent lattice path* if for all couples of enhanced steps $i \xrightarrow{a} j \prec x \xrightarrow{z} y$ with $x < j$, we have $j = z$ or $x = a$.

Now, we will study the set of coherent lattice paths of size n. First, we will prove that such lattice paths can be constructed inductively. Then, we will show that the bijection $P \mapsto \mathscr{L}(P)$ (between monotone paths and diagonal-avoiding paths) bijectively sends coherent paths on $\Delta(n, 2)$ to coherent lattice paths. Finally, our inductive construction will allow us to count the number of coherent paths on $\Delta(n, 2)$.

Theorem 4.32. *For $n \geq 3$, let $\mathcal{L}$ be a coherent lattice path of size $n+1$ and $\mathcal{L}'$ its restriction of size n. Then $\mathcal{L}'$ is coherent and $\mathcal{L}$ can be reconstructed from $\mathcal{L}'$ as it belongs to one of these (mutually exclusive) 12 cases:*

(i) if $\mathcal{L}'$ ends by a step $x \xrightarrow{n-1} n$ with $x < n-1$, then denote $\mathcal{S}' = \mathcal{S}(\mathcal{L}') \smallsetminus \{x \xrightarrow{n-1} n\}$. One of the following holds (see Figure 66):

(a) $\mathcal{S}(\mathcal{L}) = \mathcal{S}(\mathcal{L}') \cup \{n-1 \xrightarrow{n} n+1\}$

(b) $\mathcal{S}(\mathcal{L}) = \mathcal{S}(\mathcal{L}') \cup \{n \xrightarrow{n-1} n+1,\ n-1 \xrightarrow{n+1} n\}$

(c) $\mathcal{S}(\mathcal{L}) = \mathcal{S}' \cup \{x \xrightarrow{n-1} n+1,\ n-1 \xrightarrow{n+1} n\}$

(ii) if $\mathcal{L}'$ ends by steps $x \xrightarrow{y_1} n$, $y_1 \xrightarrow{n} y_2, \ldots, y_{m-1} \xrightarrow{n} y_m$ with $x < n-1$, $m \geq 3$ and $y_1 < \cdots < y_m = n-1$, then denote $\mathcal{S}' = \mathcal{S}(\mathcal{L}') \smallsetminus \{x \xrightarrow{y_1} n,\ y_1 \xrightarrow{n} y_2,\ \ldots,\ y_{m-1} \xrightarrow{n} y_m\}$. One of the following holds (see Figure 67):

(a) $\mathcal{S}(\mathcal{L}) = \mathcal{S}(\mathcal{L}') \cup \{n-1 \xrightarrow{n} n+1\}$

(b) $\mathcal{S}(\mathcal{L}) = \big(\mathcal{S}(\mathcal{L}') \smallsetminus \{y_{m-1} \xrightarrow{n} n-1\}\big) \cup \{y_{m-1} \xrightarrow{n} n+1\}$

(c) $\mathcal{S}(\mathcal{L}) = \mathcal{S}' \cup \{x \xrightarrow{y_1} n+1,\ y_1 \xrightarrow{n+1} y_2,\ \ldots,\ y_{m-1} \xrightarrow{n+1} n-1,\ n-1 \xrightarrow{n+1} n\}$

(d) $\mathcal{S}(\mathcal{L}) = \mathcal{S}' \cup \{x \xrightarrow{y_1} n+1,\ y_1 \xrightarrow{n+1} y_2,\ \ldots,\ y_{m-1} \xrightarrow{n+1} n\}$

(iii) if $\mathcal{L}'$ ends by steps $x \xrightarrow{y} n$, $y \xrightarrow{n} n-1$ with $x < n$ and $y < n-1$, then denote $\mathcal{S}' = \mathcal{S}(\mathcal{L}') \smallsetminus \{x \xrightarrow{y} n,\ y \xrightarrow{n} n-1\}$. One of the following holds (see Figure 68):

(a) $\mathcal{S}(\mathcal{L}) = \mathcal{S}(\mathcal{L}') \cup \{n-1 \xrightarrow{n} n+1\}$

(b) $\mathcal{S}(\mathcal{L}) = \big(\mathcal{S}(\mathcal{L}') \smallsetminus \{y \xrightarrow{n} n-1\}\big) \cup \{y \xrightarrow{n} n+1\}$

(c) $\mathcal{S}(\mathcal{L}) = \big(\mathcal{S}(\mathcal{L}') \smallsetminus \{y \xrightarrow{n} n-1\}\big) \cup \{n \xrightarrow{y} n+1,\ y \xrightarrow{n+1} n\}$

(d) $\mathcal{S}(\mathcal{L}) = \mathcal{S}' \cup \{x \xrightarrow{y} n+1,\ y \xrightarrow{n+1} n-1,\ n-1 \xrightarrow{n+1} n\}$

(e) $\mathcal{S}(\mathcal{L}) = \mathcal{S}' \cup \{x \xrightarrow{y} n+1,\ y \xrightarrow{n+1} n\}$

Proof. Observe first that if $\mathcal{L}$ is a coherent lattice path of size $n+1$, then its restriction $\mathcal{L}'$ of size n is also coherent. Indeed, if $i \xrightarrow{a} j \prec x \xrightarrow{z} y \in \mathcal{S}(\mathcal{L}')$ with $x < j$, then the following two properties hold:

- either $i \xrightarrow{a} j \in \mathcal{S}(\mathcal{L})$, or $i \xrightarrow{a} n+1 \in \mathcal{S}(\mathcal{L})$ and $j = n$;
- either $x \xrightarrow{z} y \in \mathcal{S}(\mathcal{L})$, or $x \xrightarrow{z} n+1 \in \mathcal{S}(\mathcal{L})$ and $y = n$, or $x \xrightarrow{n+1} y' \in \mathcal{S}(\mathcal{L})$ and $z = n$ and $y' \in \{y, n\}$.

As $\mathcal{L}$ is coherent, this implies $x = a$ or $j = z$ in all cases except if $i \xrightarrow{a} j \in \mathcal{S}(\mathcal{L})$ with $j = n$ and $x \xrightarrow{n+1} y \in \mathcal{S}(\mathcal{L})$ with $x > a$. But in the latter, $x > a > j$ and $x \neq a$, $j \neq n+1$, contradicting the coherence of $\mathcal{L}$.

Now, we first prove that all 12 cases lead to coherent paths, and then that there is no other coherent path of size $n+1$.

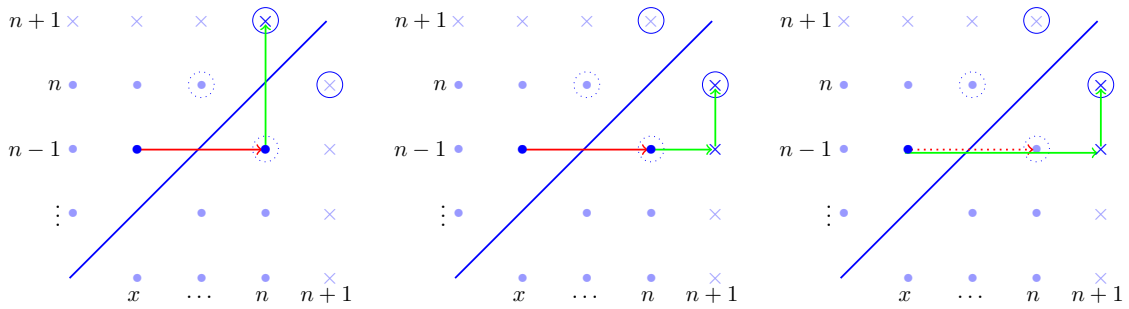

Figure 66: All 3 paths of size $n+1$ that restrict to a path of size n of type (i) in Theorem 4.32.

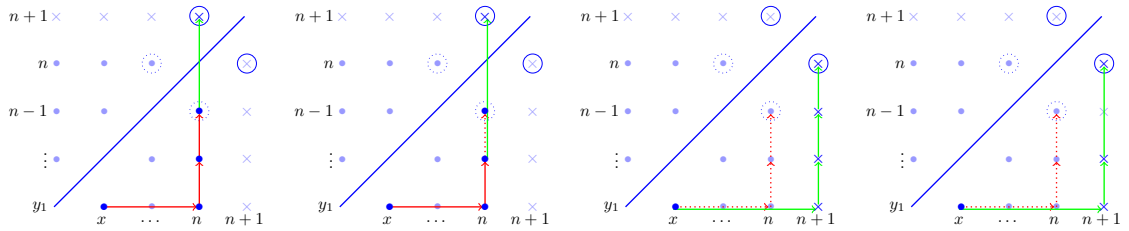

Figure 67: All 4 paths of size $n+1$ that restrict to a path of size n of type (ii) in Theorem 4.32.

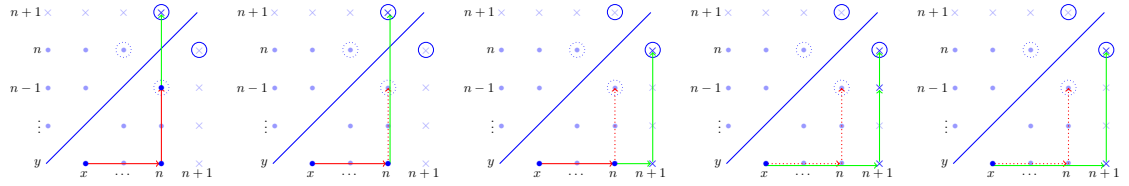

Figure 68: All 5 paths of size $n+1$ that restrict to a path of size n of type (iii) in Theorem 4.32.

We say that $i \xrightarrow{a} j \prec x \xrightarrow{z} y$ are *mutually coherent* if $x \geq j$, or if $x < j$ and $j = z$ or $x = a$.

Case $(i)(a)$, $(ii)(a)$ and $(iii)(a)$ If $i \xrightarrow{a} j \in \mathcal{S}(\mathcal{L}')$ satisfies $n-1 < j$, then $j = n$ so adding $n-1 \xrightarrow{n} n+1$ to $\mathcal{S}(\mathcal{L}')$ does not infringe coherence.

Case $(i)(b)$ $n \xrightarrow{n-1} n+1$ and $n-1 \xrightarrow{n+1} n$ are mutually coherent, and if $i \xrightarrow{a} j \in S(\mathcal{L}')$ satisfies $n-1 < j$, then $j = n$ and $a = n-1$, so $i \xrightarrow{a} j$ is mutually coherent with both $n \xrightarrow{n-1} n+1$ and $n-1 \xrightarrow{n+1} n$.

Case $(i)(c)$ and $(iii)(e)$ $x \xrightarrow{y} n+1$ and $y \xrightarrow{n+1} n$ are mutually coherent, and if $i \xrightarrow{a} j \in S'$ then $j \leq y$, so $i \xrightarrow{a} j$ is mutually coherent with both $x \xrightarrow{y} n+1$ and $y \xrightarrow{n+1} n$.

Case $(ii)(b)$ and $(iii)(b)$ Changing the endpoint of the last enhanced step doesn't interfere with mutual coherence (with previous steps).

Case $(ii)(c)$ and $(ii)(d)$ For $p \in [m-1]$, $x \xrightarrow{y_1} n+1$ and $y_p \xrightarrow{n+1} y_{p+1}$ are mutually coherent as $x \xrightarrow{y_1} n$ and $y_p \xrightarrow{n} y_{p+1}$ are in $\mathcal{S}(\mathcal{L}')$; if $i \xrightarrow{a} j \in \mathcal{S}'$, then $j \leq \max\{x, y_1\} \leq n-1$ and thus $i \xrightarrow{a} j$ is mutually coherent with $y_p \xrightarrow{n+1} y_{p+1}$, and mutually coherent with $x \xrightarrow{y_1} n+1$ as $x \xrightarrow{y_1} n \in \mathcal{S}(\mathcal{L}')$.

Case $(iii)(d)$ The above argument applies here, replacing y_1 by y.

Case $(iii)(c)$ The steps $x \xrightarrow{y} n$, $n \xrightarrow{y} n+1$ and $y \xrightarrow{n+1} n$ are mutually coherent, and if $i \xrightarrow{a} j \in \mathcal{S}(\mathcal{L}') \setminus \{y \xrightarrow{n} n-1\}$, then the above argument again applies.

Finally, we prove that there exists no other coherent paths of size $n+1$.

Case (i) If the last step of $\mathcal{L}'$ is $x \xrightarrow{n-1} n$, then the 3 claimed $\mathcal{L}$ are the only diagonal-avoiding lattice paths whose restriction is $\mathcal{L}'$ (as lattice paths must be North-East increasing).

Case (ii) If $\mathcal{L}$ restrict to $\mathcal{L}'$ whose last steps are $x \xrightarrow{y_1} n$, $y_1 \xrightarrow{n} y_2, \dots, y_{m-1} \xrightarrow{n} y_m$ with $x < n-1$, $m \geq 3$ and $y_1 < \cdots < y_m = n-1$, then consider the last step of the form $i \xrightarrow{a} n+1$ in $\mathcal{L}$. Either $a = n$ and $\mathcal{L}$ is necessarily in cases (a) or (b); or $(i, a) \in \{(x, y_1)\} \cup \{(n, y_p)\}_{p \in [m]}$. The first possibility leads necessarily to cases (c) and (d), while the latest lead to non-coherent paths, as $x \xrightarrow{y_1} n$ would be in $\mathcal{L}$ and is not mutually coherent with $y_p \xrightarrow{n+1} y_{p+1}$ for $p \geq 2$.

Case (iii) If the last steps of $\mathcal{L}'$ are $x \xrightarrow{n-1} n$ and $y \xrightarrow{n} n-1$, then there are 6 diagonal-avoiding lattice paths whose restriction is $\mathcal{L}'$ (as lattice paths must be North-East increasing). The only non-coherent one is given by $\mathcal{S}(\mathcal{L}) = \big(\mathcal{S}(\mathcal{L}') \setminus \{y \xrightarrow{n} n-1\}\big) \cup \{n \xrightarrow{y} n+1,\ y \xrightarrow{n+1} n-1,\ n-1 \xrightarrow{n+1} n\}$, which is not coherent as $n \xrightarrow{y} n+1$ and $n-1 \xrightarrow{n+1} n$ are not mutually coherent (as $y < n-1$). □

Now that we know how to inductively construct all coherent lattice paths, we are able to prove the reciprocal of Theorem 4.24. The proof of the following theorem will be cumbersome but not difficult: for each 12 cases of Theorem 4.32, we are going to exhibit a vector $\boldsymbol{\omega}$ that captures it.

Theorem 4.33. *Coherent paths on $\Delta(n, 2)$ are in bijection with coherent lattice paths of size n.*

Proof. Theorem 4.24 proves that the application $\mathscr{L}$ sends injectively coherent paths on $\Delta(n, 2)$ to coherent lattice paths of size n. We now prove the converse: if $\mathcal{L}$ is a coherent lattice path of size n, then there exists a coherent path P on $\Delta(n, 2)$ such that $\mathscr{L}(P) = \mathcal{L}$. To this end, we will use the induction process of Theorem 4.32. Thanks to Example 4.29, we know that all coherent lattice paths of size 3 and 4 are coherent paths on $\Delta(3, 2)$ and $\Delta(4, 2)$. We are going to prove that if $\mathcal{L}' = \mathscr{L}(P')$ for $\mathcal{L}'$ a coherent lattice path of size n, then for all coherent path $\mathcal{L}$ of size $n+1$ such that $\mathcal{L}$ restrict to $\mathcal{L}'$ (*i.e.* in all 12 cases of Theorem 4.32), we can find a coherent path P on $\Delta(n+1, 2)$ such that $\mathcal{L} = \mathscr{L}(P)$.

Let $\mathcal{L}'$ be a coherent lattice path of size n such that $\mathcal{L}' = \mathscr{L}(P')$ where P' is a coherent path and $\boldsymbol{\omega}' \in \mathbb{R}^n$ captures P'. We are going to find ω_{n+1} such that $\boldsymbol{\omega} := (\omega'_1, \dots, \omega'_n, \omega_{n+1}) \in \mathbb{R}^{n+1}$ captures a path P with $\mathscr{L}(P) = \mathcal{L}$ (in some cases, we will also modify ω_n slightly). We denote $\tau_{\boldsymbol{\omega}}(i \to j) = \frac{\omega_j - \omega_i}{c_j - c_i}$ as usual. As we will focus the behavior of the points $(c_i + c_j, \omega_i + \omega_{+j})$ for $(i, j) \in \mathcal{L}$, in order to ease notation, we say "the point (i, j)" instead of "the point $(c_i + c_j, \omega_i + \omega_j)$". We will distinguish three cases following the main cases of Theorem 4.32.

Case (i) Suppose the last step of $\mathcal{L}'$ is $x \xrightarrow{n-1} n$ with $x < n-1$. Remark that for $i \notin \{x, n-1, n\}$:

$$\tau_{\boldsymbol{\omega}}(n-1 \to n) < \tau_{\boldsymbol{\omega}}(x \to n) < \tau_{\boldsymbol{\omega}}(i \to n)$$

Indeed, the first inequality comes directly from the last step of $\mathcal{L}'$: if the inequality were reversed, the last step would have been $n-1 \xrightarrow{x} n$ instead. The second inequality follows from Lemma 4.25 applied to the triangle $(x, n-1)$, $(i, n-1)$, $(n, n-1)$.

Note first that, for $i < n$, if ω_{n+1} satisfies that $\tau_{\boldsymbol{\omega}}(n \to n+1) < \tau_{\boldsymbol{\omega}}(i \to n)$, then there can not be a step $i \xrightarrow{a} n+1$ in $\mathcal{S}(P)$ as $\tau_{\boldsymbol{\omega}}(i \to n+1) < \tau_{\boldsymbol{\omega}}(i \to n)$ by Lemma 4.25, thus the points associated to $(i, n+1)$ are all below the path P' and do not belong to P. As $\tau_{\boldsymbol{\omega}}(n \to n+1)$ is a continuous increasing function of ω_{n+1}, this gives three regimes.

Case $(i)(a)$: To obtain P with $\mathscr{L}(P)$ of form $(i)(a)$ in Theorem 4.32, choose ω_{n+1} small enough to satisfy $\tau_{\boldsymbol{\omega}}(n \to n+1) < \tau_{\boldsymbol{\omega}}(n-1 \to n)$, then the path P captured by $\boldsymbol{\omega}$ has $\mathcal{S}(P') \subset \mathcal{S}(P)$ by the above, and $n-1 \xrightarrow{n} n+1 \in \mathcal{S}(P)$ by applying Lemma 4.25 in the triangle $(n, n-1)$, $(n-1, n+1)$, $(n, n+1)$.

Case $(i)(b)$: To obtain P with $\mathscr{L}(P)$ of form $(i)(b)$ in Theorem 4.32, choose ω_{n+1} to satisfy $\tau_{\boldsymbol{\omega}}(n-1 \to n) < \tau_{\boldsymbol{\omega}}(n \to n+1) < \tau_{\boldsymbol{\omega}}(x \to n)$, then the path P captured by $\boldsymbol{\omega}$ has $\mathcal{S}(P') \subset \mathcal{S}(P)$ by the above, and $n \xrightarrow{n-1} n+1 \in \mathcal{S}(P)$ and $n-1 \xrightarrow{n+1} n \in \mathcal{S}(P)$ by applying Lemma 4.25 to the triangle $(n, n-1)$, $(n-1, n+1)$, $(n, n+1)$.

Case $(i)(c)$: To obtain P with $\mathscr{L}(P)$ of form $(i)(c)$ in Theorem 4.32, choose ω_{n+1} to satisfy $\tau_{\boldsymbol{\omega}}(x \to n) < \tau_{\boldsymbol{\omega}}(n \to n+1) < \min_{i \notin \{x,n\}} \tau_{\boldsymbol{\omega}}(i \to n)$, then the path P captured by $\boldsymbol{\omega}$ has $\mathcal{S}(P') \setminus \{x \xrightarrow{n-1} n\} \subset \mathcal{S}(P)$ by the above, and $x \xrightarrow{n-1} n+1 \in \mathcal{S}(P)$ and $n-1 \xrightarrow{n+1} n \in \mathcal{S}(P)$.

We have shown that if $\mathcal{L}'$ is in the case (i), then all the paths $\mathcal{L}$ that restrict to $\mathcal{L}'$ are of the form $\mathcal{L} = \mathscr{L}(P)$ for some coherent P.

Case (ii) Suppose the last steps of $\mathcal{L}'$ are $x \xrightarrow{y_1} n, y_1 \xrightarrow{n} y_2, \ldots, y_{m-1} \xrightarrow{n} n-1$ with $m \geq 3$. Then for all $i \notin \{x, y_1, n\}$, by the same argument as before:

$$\tau_{\boldsymbol{\omega}}(y_{m-1} \to n-1) < \tau_{\boldsymbol{\omega}}(y_{m-2} \to y_{m-1}) < \cdots < \tau_{\boldsymbol{\omega}}(y_1 \to y_2) < \tau_{\boldsymbol{\omega}}(x \to n) < \tau_{\boldsymbol{\omega}}(i \to n)$$

We distinguish three regimes.

Case $(ii)(a)$: To obtain P with $\mathscr{L}(P)$ of form $(ii)(a)$ in Theorem 4.32, choose ω_{n+1} small enough to satisfy $\tau_{\boldsymbol{\omega}}(n \to n+1) < \tau_{\boldsymbol{\omega}}(y_{m-1} \to n-1)$, then the path P captured by $\boldsymbol{\omega}$ has $\mathcal{S}(P') \subset \mathcal{S}(P)$, and $n-1 \xrightarrow{n} n+1 \in \mathcal{S}(P)$ by applying Lemma 4.25 to the triangle $(n, n-1)$, $(n-1, n+1)$ and $(n, n+1)$.

Case $(ii)(b)$: To obtain P with $\mathscr{L}(P)$ of form $(ii)(b)$ in Theorem 4.32, choose ω_{n+1} to satisfy $\tau_{\boldsymbol{\omega}}(y_{m-1} \to n-1) < \tau_{\boldsymbol{\omega}}(n \to n+1) < \tau_{\boldsymbol{\omega}}(y_{m-2} \to y_{m-1})$, then the path P captured by $\boldsymbol{\omega}$ has $\mathcal{S}(P') \setminus \{y_{m-1} \xrightarrow{n} n-1\} \subset \mathcal{S}(P)$, and $y_{m-1} \xrightarrow{n} n+1 \in \mathcal{S}(P)$ because applying Lemma 4.25 to the triangle (y_{m-1}, n), $(n, n-1)$ and $(n-1, n+1)$ gives that $\tau_{\boldsymbol{\omega}}(n-1 \to n+1) < \tau_{\boldsymbol{\omega}}(n-1 \to n)$, and applying it to (y_{m-1}, n), $(y_{m-1}, n+1)$ and $(n, n+1)$ gives that $\tau_{\boldsymbol{\omega}}(y_{m-1} \to n+1) > \tau_{\boldsymbol{\omega}}(n \to n+1)$.

Case $(ii)(d)$: To obtain P with $\mathscr{L}(P)$ of form $(ii)(d)$ in Theorem 4.32, choose ω_{n+1} to satisfy $\tau_{\boldsymbol{\omega}}(x \to n) < \tau_{\boldsymbol{\omega}}(n \to n+1) < \min_{i \notin \{x,n\}} \tau_{\boldsymbol{\omega}}(i \to n)$, then the path P captured by $\boldsymbol{\omega}$ has $\mathcal{S}' \subset \mathcal{S}(P)$, and by applying Lemma 4.25 to the triangle (x, y_1), (n, y_1) and $(n+1, y_1)$, one gets that $x \xrightarrow{y_1} n+1 \in \mathcal{S}(P)$. Moreover, the projected path $\big((n+1, y_1), (n+1, y_2), \ldots, (n+1, y_{m-1}), (n+1, n-1)\big)$ is parallel and higher than the projected path $\big((n, y_1), (n, y_2), \ldots, (n, y_{m-1}), (n, n-1)\big)$, thus $y_i \xrightarrow{n+1} y_{i+1} \in \mathcal{S}(P)$ for $i \in [1, m-2]$. As $\tau_{\boldsymbol{\omega}}(y_{m-1} \to n-1) < \tau_{\boldsymbol{\omega}}(x \to n) \leq \tau_{\boldsymbol{\omega}}(n-1 \to n)$ in P', Lemma 4.25 ensures that $y_{m-1} \xrightarrow{n+1} n \in \mathcal{S}(P)$.

Case $(ii)(c)$: To obtain P with $\mathscr{L}(P)$ of form $(ii)(c)$ in Theorem 4.32, note that in the previous sub-case there is no point (i, n) in P except from $(n, n+1)$. So lowering the value of ω_n (with the same fixed ω_{n+1} as in the previous sub-case) will not affect the path except in the last triangle $(y_{m-1}, n+1)$, $(n-1, n+1)$, $(n, n+1)$. Taking ω_n low enough to satisfy $\tau_{\boldsymbol{\omega}}(y_{m-1} \to n-1) > \tau_{\boldsymbol{\omega}}(n-1 \to n)$, we obtain a path $\tilde{P}$ with $\mathcal{S}(P) \setminus \{y_{m-1} \xrightarrow{n+1} n\} \subset \mathcal{S}(\tilde{P})$ and $\{y_{m-1} \xrightarrow{n+1} n-1,\ n-1 \xrightarrow{n+1} n\} \in \mathcal{S}(\tilde{P})$.

Case (*iii*) Suppose that the last steps of $\mathcal{L}'$ are $x \xrightarrow{n} y$, $y \xrightarrow{n} n-1$. Then for $i \notin \{x, y, n\}$:

$$\tau_{\boldsymbol{\omega}}(y \to n-1) < \tau_{\boldsymbol{\omega}}(y \to n) < \tau_{\boldsymbol{\omega}}(x \to n) < \tau_{\boldsymbol{\omega}}(i \to n)$$

Indeed, $\tau_{\boldsymbol{\omega}}(y \to n) < \tau_{\boldsymbol{\omega}}(x \to n)$ otherwise $x \xrightarrow{y} n \notin \mathcal{S}(P')$, and $\tau_{\boldsymbol{\omega}}(y \to n-1) < \tau_{\boldsymbol{\omega}}(y \to n)$ as already $\tau_{\boldsymbol{\omega}}(y \to n-1) < \tau_{\boldsymbol{\omega}}(n-1 \to n)$.

Case (*iii*)(*a*)*:* To obtain P with $\mathscr{L}(P)$ of form (*iii*)(*a*) in Theorem 4.32, choose ω_{n+1} small enough to satisfy $\tau_{\boldsymbol{\omega}}(n \to n+1) < \tau_{\boldsymbol{\omega}}(y \to n-1)$, then $\mathcal{S}(P') \subset \mathcal{S}(P)$ and $n-1 \xrightarrow{n} n+1 \in \mathcal{S}(P)$.

Case (*iii*)(*b*)*:* To obtain P with $\mathscr{L}(P)$ of form (*iii*)(*b*) in Theorem 4.32, choose ω_{n+1} to satisfy $\tau_{\boldsymbol{\omega}}(y \to n-1) < \tau_{\boldsymbol{\omega}}(n \to n+1) < \tau_{\boldsymbol{\omega}}(y \to n)$, then $\mathcal{S}(P') \setminus \{y \xrightarrow{n} n-1\} \subset \mathcal{S}(P)$, and as $\tau_{\boldsymbol{\omega}}(n \to n+1) < \tau_{\boldsymbol{\omega}}(y \to n)$, Lemma 4.25 ensures $y \xrightarrow{n} n+1 \in \mathcal{S}(P)$.

Case (*iii*)(*c*)*:* To obtain P with $\mathscr{L}(P)$ of form (*iii*)(*c*) in Theorem 4.32, choose ω_{n+1} to satisfy $\tau_{\boldsymbol{\omega}}(y \to n) < \tau_{\boldsymbol{\omega}}(n \to n+1) < \tau_{\boldsymbol{\omega}}(x \to n)$, then $\mathcal{S}(P') \setminus \{y \xrightarrow{n} n-1\} \subset \mathcal{S}(P)$, and as $\tau_{\boldsymbol{\omega}}(n \to n+1) > \tau_{\boldsymbol{\omega}}(y \to n)$, Lemma 4.25 ensures $\{n \xrightarrow{y} n+1,\ y \xrightarrow{n+1} n\} \subset \mathcal{S}(P)$.

Case (*iii*)(*e*)*:* To obtain P with $\mathscr{L}(P)$ of form (*iii*)(*e*) in Theorem 4.32, choose ω_{n+1} to satisfy $\tau_{\boldsymbol{\omega}}(x \to n) < \tau_{\boldsymbol{\omega}}(n \to n+1) < \min_{i \notin \{x,n\}} \tau_{\boldsymbol{\omega}}(i \to n)$, then $\mathcal{S}' \cup \{x \xrightarrow{y} n+1\} \subset \mathcal{S}(P)$, and $y \xrightarrow{n} n+1 \in \mathcal{S}(P)$ as $\tau_{\boldsymbol{\omega}}(y \to n-1) < \tau_{\boldsymbol{\omega}}(n-1 \to n)$.

Case (*iii*)(*d*)*:* To obtain P with $\mathscr{L}(P)$ of form (*iii*)(*d*) in Theorem 4.32, from the previous value of ω_{n+1}, we lower the value of ω_n until $\tau_{\boldsymbol{\omega}}(y \to n-1) > \tau_{\boldsymbol{\omega}}(n-1 \to n)$. As no other point of the form (i, n) belongs to P, this new $\boldsymbol{\omega}$ captures a path $\tilde{P}$ with $\mathcal{S}(P) \setminus \{y \xrightarrow{n+1} n\} \subset \mathcal{S}(\tilde{P})$ and $\{y \xrightarrow{n+1} n-1,\ n-1 \xrightarrow{n+1} n\} \subset \mathcal{S}(\tilde{P})$.

We have proven that in all 12 cases, if the restriction of $\mathcal{L}$ is the image by $\mathscr{L}$ of a coherent path on $\Delta(n-1, 2)$, then $\mathcal{L}$ is the image by $\mathscr{L}$ of a coherent path on $\Delta(n, 2)$. This shows the surjectivity of $\mathscr{L}$. □

4.2.4 Counting the number of coherent monotone paths on $\Delta(n, 2)$

The induction process of Theorem 4.32 allows us to count precisely the number of coherent lattice paths, which is the number of vertices of $\mathsf{M}(n, 2)$ thanks to Theorem 4.33.

Let t_n be the number of coherent paths $\mathcal{L}$ of size n such that the last step of $\mathcal{L}$ is $x \xrightarrow{n-1} n$ (*i.e.* of type (*i*) in Theorem 4.32). Let q_n be the number of these finishing by steps $x \xrightarrow{y_1} n, y_1 \xrightarrow{n} y_2, \ldots, y_{m-1} \xrightarrow{n} n-1$ with $m \geq 3$ (*i.e.* of type (*ii*) in Theorem 4.32). Let c_n be the number of these finishing by $x \xrightarrow{y} n, y \xrightarrow{n} n-1$ (*i.e.* of type (*iii*) in Theorem 4.32).

Observing the induction process of Theorem 4.32 gives the following:

Proposition 4.34. *The sequences t_n, q_n and c_n satisfy the following recursive formula:*

$$\forall n \geq 4,\ \begin{pmatrix} t_{n+1} \\ q_{n+1} \\ c_{n+1} \end{pmatrix} = M \begin{pmatrix} t_n \\ q_n \\ c_n \end{pmatrix} \quad \textit{with} \quad M = \begin{pmatrix} 1 & 2 & 2 \\ 0 & 2 & 1 \\ 2 & 0 & 2 \end{pmatrix} \quad \textit{and} \quad \begin{pmatrix} t_4 \\ q_4 \\ c_4 \end{pmatrix} = \begin{pmatrix} 3 \\ 1 \\ 4 \end{pmatrix}$$

Proof. The values for t_4, q_4 and c_4 follow from Example 4.29.

Looking at the induction process in Theorem 4.32, for each case (*i*)(*a*) to (*iii*)(*e*), one can identify if the created coherent path of size $n+1$ is of the type of case (*i*), (*ii*) or (*iii*). For example, if $\mathcal{L}'$ of size n ends by a step $x \xrightarrow{n-1} n$, then there are three $\mathcal{L}$ of size $n+1$ that restrict to $\mathcal{L}'$: in case (*i*)(*a*), $\mathcal{L}$ ends with $y \xrightarrow{n} n+1$ (with $y = n-1$) so it belongs to type (*i*). The case analysis is summarized in the following table:

	(*a*)	(*b*)	(*c*)	(*d*)	(*e*)
(*i*)	(*i*)	(*iii*)	(*iii*)		
(*ii*)	(*i*)	(*i*)	(*ii*)	(*ii*)	
(*iii*)	(*i*)	(*i*)	(*iii*)	(*ii*)	(*iii*)

Reading off the table gives the matrix M. □

Theorem 4.35. *For $n \geq 4$, there are $\frac{1}{3}\left(25 \times 4^{n-4} - 1\right)$ coherent paths of size n.*

Proof. By definition, the total number of coherent paths of size n is $t_n + q_n + c_n$.

A quick analysis of M shows that $\mathrm{Sp}(M) = \{0, 1, 4\}$ with $(2, -2, -1)M = (0, 0, 0)$. Thus for all n: $2t_n = 2q_n + c_n$. It follows that if $c_n = t_n + 1$, then $t_n = 2q_n + 1$ and thus $c_{n+1} = 2t_n + 2c_n = t_n + 2q_n + 2c_n + 1 = t_{n+1} + 1$. By induction: $\forall n \geq 4, c_n = t_n + 1$. This gives: $t_{n+1} + q_{n+1} + c_{n+1} = 4(t_n + q_n + c_n) + 1$

With $t_4 + q_4 + c_4 = 8$, this recursive formula gives the number of coherent paths of size n. □

This formula solves the question we started with: determine the vertices of $\mathsf{M}(n, 2)$ and count them. Notwithstanding, one can go even further in the analysis of the induction process. Let $t_{n,\ell}$ be the number of coherent path of size n and length ℓ that end with a step $x \xrightarrow{n-1} n$ and let $q_{n,\ell}$, $c_{n,\ell}$ be the counterparts for the two other main cases of the induction. Let $T_n = \sum_\ell t_{n,\ell} z^\ell$, $Q_n = \sum_\ell q_{n,\ell} z^\ell$ and $C_n = \sum_\ell c_{n,\ell} z^\ell$ be the associated generating polynomials, then observing Theorem 4.32 gives the following:

Proposition 4.36. *The sequences of polynomials T_n, Q_n and C_n satisfy the following recursive formula:*

$$\forall n \geq 4,\ \begin{pmatrix} T_{n+1} \\ Q_{n+1} \\ C_{n+1} \end{pmatrix} = \mathcal{M} \begin{pmatrix} T_n \\ Q_n \\ C_n \end{pmatrix} \quad \textit{with} \quad \mathcal{M} = \begin{pmatrix} z & 1+z & 1+z \\ 0 & 1+z & z \\ z+z^2 & 0 & 1+z \end{pmatrix}, \quad \begin{pmatrix} T_4 \\ Q_4 \\ C_4 \end{pmatrix} = \begin{pmatrix} z^4 + 2z^3 \\ z^4 \\ 2z^4 + 2z^3 \end{pmatrix}$$

Remark 4.37. Note that evaluating the previous relation at $z = 1$ gives back Proposition 4.34.

Proof of Proposition 4.36. The values for T_4, Q_4 and C_4 have been explored in Example 4.29.

Looking at the induction process, for each case $(i)(a)$ to $(iii)(e)$, one can identify the length of the created coherent path of size $n+1$. For example, if $\mathcal{L}'$ of size n and length ℓ ends by a step $x \xrightarrow{n-1} n$, then there are three $\mathcal{L}$ of size $n+1$ that restricts to $\mathcal{L}'$: in case $(i)(a)$, $\mathcal{L}$ contains 1 step more than $\mathcal{L}'$ so it has length $\ell + 1$. The case analysis is summarized in the following table, assuming the restricted path is of length ℓ:

	(a)	(b)	(c)	(d)	(e)
(i)	$\ell+1$	$\ell+2$	$\ell+1$		
(ii)	$\ell+1$	ℓ	$\ell+1$	ℓ	
(iii)	$\ell+1$	ℓ	$\ell+1$	$\ell+1$	ℓ

Reading off this table together with the one of the proof of Proposition 4.34 yields $\mathcal{M}$. □

The matrix $\mathcal{M}$ (over the polynomial ring) has three eigenvalues $\lambda_0 = 0$, $\lambda_+ = 1 + \frac{3}{2}z + \frac{1}{2}z\sqrt{4z+5}$, and $\lambda_- = 1 + \frac{3}{2}z - \frac{1}{2}z\sqrt{4z+5}$ with associated (left) eigenvectors:

$$\boldsymbol{x}_0 = \begin{pmatrix} -1 & 1 & \frac{1}{1+z} \end{pmatrix}, \ \boldsymbol{x}_+ = \begin{pmatrix} 1 & \frac{\sqrt{4z+5}-1}{2z} & \frac{z\sqrt{4z+5}+z+2}{2(z^2+z)} \end{pmatrix}, \ \boldsymbol{x}_- = \begin{pmatrix} 1 & -\frac{\sqrt{4z+5}+1}{2z} & \frac{-z\sqrt{4z+5}+z+2}{2(z^2+z)} \end{pmatrix}$$

Unfortunately, the square roots in the eigenvalues and eigenvectors make it very difficult to derive an explicit formula as simple as in Theorem 4.35, but we can prove two very interesting properties on the number of coherent paths of a given length.

Theorem 4.38. *For a fixed size n with $n \geq 4$, the longest coherent path of size n is of length $\ell_{\max} = \left\lfloor \frac{3}{2}(n-1) \right\rfloor$. The number of coherent paths of size n and length $\ell_{\max}$ is 1 if n is odd, and $\left\lfloor \frac{3}{2}(n-1) \right\rfloor$ if n is even.*

Proof. We will prove by induction the slightly stronger following statement on the degrees and leading coefficients of T_n, Q_n and C_n. Denote $\nu_n = \left\lfloor \frac{3}{2}(n-1) \right\rfloor$:

$$\begin{cases} \text{if } n \text{ odd}, & T_n = (\nu_n - 2)z^{\nu_n - 1} + o(z^{\nu_n - 1}), & Q_n = O(z^{\nu_n - 1}), & C_n = z^{\nu_n} + o(z^{\nu_n}) \\ \text{if } n \text{ even}, & T_n = z^{\nu_n} + o(z^{\nu_n}), & Q_n = z^{\nu_n} + o(z^{\nu_n}), & C_n = (\nu_n - 2)z^{\nu_n} + o(z^{\nu_n}) \end{cases}$$

This statement holds for $n = 4$ as $\nu_4 = 4$, $T_4 = z^4 + o(z^4)$, $Q_4 = z^4$ and $C_4 = 2z^4 + o(z^4)$. Now, it is just a matter of multiplying by $\mathcal{M}$. Suppose n is odd and the statement holds, then:

$$\begin{aligned} T_{n+1} &= zT_n + (1+z)Q_n + (1+z)C_n \\ &= O(z^{\nu_n}) + O(z^{\nu_n}) + z^{\nu_n+1} + o(z^{\nu_n+1}) \\ &= z^{\nu_{n+1}} + o(z^{\nu_{n+1}}) && \text{as } \nu_{n+1} = \nu_n + 1 \end{aligned}$$

$$\begin{aligned} Q_{n+1} &= (1+z)Q_n + zC_n \\ &= O(z^{\nu_n}) + z^{\nu_n+1} + o(z^{\nu_n+1}) \\ &= z^{\nu_{n+1}} + o(z^{\nu_{n+1}}) && \text{as } \nu_{n+1} = \nu_n + 1 \end{aligned}$$

$$\begin{aligned} C_{n+1} &= (z^2+z)T_n + (1+z)C_n \\ &= (\nu_n - 2)z^{\nu_n+1} + o(z^{\nu_n+1}) + z^{\nu_n+1} + o(z^{\nu_n+1}) \\ &= (\nu_{n+1} - 2)z^{\nu_{n+1}} + o(z^{\nu_{n+1}}) && \text{as } \nu_{n+1} = \nu_n + 1 \end{aligned}$$

Suppose n is even, and the statement holds, then:

$$\begin{aligned} T_{n+1} &= zT_n + (1+z)Q_n + (1+z)C_n \\ &= z^{\nu_n+1} + z^{\nu_n+1} + (\nu_n - 2)z^{\nu_n+1} + o(z^{\nu_n+1}) \\ &= (\nu_{n+1} - 2)z^{\nu_{n+1}-1} + o(z^{\nu_{n+1}-1}) && \text{as } \nu_{n+1} = \nu_n + 2 \end{aligned}$$

$$\begin{aligned} Q_{n+1} &= (1+z)Q_n + zC_n \\ &= O(z^{\nu_n+1}) + O(z^{\nu_n+1}) \\ &= O(z^{\nu_{n+1}-1}) && \text{as } \nu_{n+1} = \nu_n + 2 \end{aligned}$$

$$\begin{aligned} C_{n+1} &= (z^2+z)T_n + (1+z)C_n \\ &= z^{\nu_n+2} + o(z^{\nu_n+2}) + O(z^{\nu_n+1}) \\ &= z^{\nu_{n+1}} + o(z^{\nu_{n+1}}) && \text{as } \nu_{n+1} = \nu_n + 2 \end{aligned}$$

Thus, by induction the polynomial $T_n + Q_n + C_n$ has degree ν_n and leading coefficient 1 if n is odd, and ν_n if n is even, which proves the theorem. □

Theorem 4.39. *For a fixed length ℓ, the number of coherent paths of size $n \geq \left\lceil \frac{2}{3}\ell + 1 \right\rceil$ is a polynomial in n of degree $\ell - 3$.*

Proof. Let $v_{n,\ell}$ be the total number of coherent paths of size n and length ℓ, then $V_n = \sum_\ell v_{n,\ell} z^\ell = T_n + Q_n + C_n$. We can compute V_n thanks to the powers of $\mathcal{M}$:

$$V_{n+4} = \begin{pmatrix} 1 & 1 & 1 \end{pmatrix} \mathcal{M}^n \begin{pmatrix} T_4 \\ Q_4 \\ C_4 \end{pmatrix}$$

With the eigenvalues and eigenvectors given above, one can compute:

$$V_{n+4} = \frac{\lambda_+^n - \lambda_-^n}{\sqrt{4z+5}} z^5 + \left(2(\lambda_+^n + \lambda_-^n) + 6\frac{\lambda_+^n - \lambda_-^n}{\sqrt{4z+5}} \right)(z^4 + z^3)$$

Note that as λ_+ and λ_- depend on z. Indeed:

$$\frac{\lambda_+^n - \lambda_-^n}{\sqrt{4z+5}} = \sum_k \binom{n}{2k+1} \left(1 + \frac{3}{2}z\right)^{n-(2k+1)} \left(\frac{5}{4} + z\right)^k z^{2k+1}$$

and

$$\lambda_+^n + \lambda_-^n = 2\sum_k \binom{n}{2k} \left(1 + \frac{3}{2}z\right)^{n-2k} \left(\frac{5}{4} + z\right)^k z^{2k}$$

Not only they are polynomials in z (which was expected as V_n is a polynomial by definition), but we can investigate their coefficients. It allows us to re-write:

$$V_{n+4} = \sum_{(a,b,c)\in\mathbb{N}^3} \alpha_{n,a,b,c} \left(1+\frac{3}{2}z\right)^a \left(\frac{5}{4}+z\right)^b z^c$$

where $\alpha_{n,a,b,c}$ is a sum of binomial coefficient $\binom{n}{f(a,b,c)}$ with f a function of a, b and c. This coefficient is thus a polynomial in n.

By Theorem 4.38, we know that the polynomial V_n has degree $\left\lfloor \frac{3}{2}(n-1) \right\rfloor$, thus for a fixed ℓ, the coefficient of V_n on z^ℓ is non-zero when $n \geq \left\lceil \frac{2}{3}\ell + 1 \right\rceil$. This coefficient can be seen as (a multiple of) the evaluation at $z=0$ of the polynomial $\frac{\partial^\ell}{\partial z^\ell} V_n$. But this derivative is again a sum of (products of) powers of $\left(1+\frac{3}{2}z\right)$, of $\left(\frac{5}{4}+z\right)$ and of z, with no new dependencies in n. Evaluating at $z=0$ gives that $v_{n,\ell}$ is a sum (which coefficients depend on ℓ) of $\binom{n}{f(a,b,c)}$: a polynomial in n.

To obtain the degree of this polynomial, we look for the greatest κ such that $\binom{n}{\kappa}$ appears in the coefficient of z^ℓ. In the developments of both $\frac{\lambda_+^n - \lambda_-^n}{\sqrt{4z+5}}$ and $\left(\lambda_+^n + \lambda_-^n\right)$, remark that κ is the power on the factor z. For a fixed ℓ, the greatest power on the factor z appearing in $\frac{\lambda_+^n - \lambda_-^n}{\sqrt{4z+5}} z^5$ is $\ell - 5$, the greatest in $\left(2(\lambda_+^n + \lambda_-^n) + 6\frac{\lambda_+^n - \lambda_-^n}{\sqrt{4z+5}}\right)(z^4+z^3)$ is $\ell-3$. Thus, the degree of the polynomial $v_{n,\ell}$, as a polynomial in n, is $\ell - 3$. □

Example 4.40. With the help of Proposition 4.36, one can compute the number of coherent paths of size n and length ℓ:

$n\vert\ell$	3	4	5	6	7	8	9	10	11	12	13	14	15
4	4	4											
5	4	16	12	1									
6	4	28	56	38	7								
7	4	40	132	195	129	32	1						
8	4	52	240	556	694	448	129	10					
9	4	64	380	1205	2250	2496	1571	501	61	1			
10	4	76	552	2226	5565	8896	9019	5564	1914	304	13		
11	4	88	756	3703	11627	21416	34622	32725	19881	7236	1375	99	1

In this table, one can read out Theorem 4.38 (for $n \leq 11$) by looking at the right-most value in each line. Furthermore, Theorem 4.39 ensures that each column ℓ is a polynomial in n of degree $\ell - 3$, observing the rows given, the following holds for $n \geq 1$:

- for $\ell = 3$: $v_{n+3,3} = 4$ is also the number of diagonal-avoiding paths of length 3.
- for $\ell = 4$: $v_{n+3,4} = 12n - 8$ is also the number of diagonal-avoiding paths of length 4.
- for $\ell = 5$: $v_{n+4,5} = 4n(4n-1)$ is **not** the number of diagonal-avoiding paths of length 5.
- for $\ell = 6$: $v_{n+5,6} = 14n^3 - 24n^2 + 11n$.
- for $\ell = 7$: $v_{n+6,7} = \frac{1}{6}(55n^4 - 2n^3 - 34n^2 + 23n)$.

And one can easily continue this list with a computer.

4.2.5 Perspectives and open questions

Computational remarks As usual, all the objects present in this section have been implemented with Sage. Namely, I am able to compute monotone path polytopes and label their vertices by the corresponding monotone paths and their normal cones (*i.e.* the cone of $\boldsymbol{\omega}$ that captures the

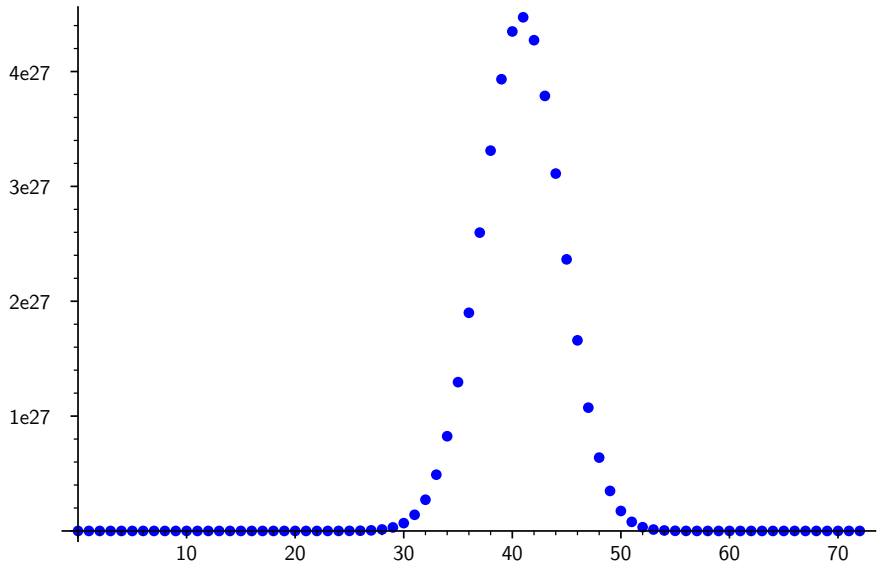

Figure 69: Number of coherent paths on $\Delta(50, 2)$ for length $\ell \in [3, 73]$

corresponding monotone path). Monotone path polytopes are computed as a Minkowski sum of sections, one at each vertex, however the same remark as for max-slope pivot rule polytopes holds: computing Minkowski sums in high dimension and with a lot of vertices takes time.

Furthermore, in the case of the monotone path polytope of the hypersimplices $\Delta(n, 2)$, all numerical statements have been checked by (i) constructing the monotone path polytope and counting its vertices (up to dimension 8); (ii) constructing all possible monotone paths and solving the linear system to know whether it can be captured or not (up to dimension 9); (iii) generating all paths that respect the criterion of Theorem 4.24 and verifying if they are coherent (up to dimension 12); (iv) implementing the matrix recursion (up to dimension 300). Fortunately, all these methods lead to the same result. We also have implemented similar methods for counting the paths by their length.

Besides, the diagonalization of matrices were done with the help of Sage (and latter checked by hand and with Wolfram Alpha), which benefits from excellent and easy-to-use tools to deal with matrices over any rings (especially the ring of symbolic expressions, *i.e.* of polynomials and more).

Assets and limits of the current approach, open questions We have detailed the behavior of $v_{n,\ell}$ for a fixed length ℓ. But on the other side, for a fixed size n, one can look at the sequence $\big(v_{n,\ell}\ ;\ \ell \in [3, \lfloor \frac{3}{2}(n-1) \rfloor]\big)$. Jesús De Loera conjectured the following for all polytopes:

Conjecture 4.41 (De Loera)**.** *For any polytope* P *and generic objective function* $\mathbf{c}$*, the sequence* $\big(N_\ell\ ;\ \ell \geq 1\big)$ *of the number of coherent monotone paths on* P *of length* ℓ *is a log-concave sequence.*

Especially, in our case, this conjectures states that for a fixed dimension n, the sequence $\big(v_{n,\ell}\ ;\ \ell \geq 3\big)$ is log-concave. Thanks to Proposition 4.36, we can compute these sequences for large n, for example $n = 50$ in Figure 69. All the computations done so far tend to confirm this conjecture, in particular it holds true for all $n \leq 150$. Moreover, note that the archetypal sequence $\big(\binom{n}{\ell}\ ;\ \ell \in [0, n]\big)$ is log-concave and shares a property similar to Theorem 4.39: for a fixed ℓ, the value $\binom{n}{\ell}$ is a polynomial in n of degree ℓ. Even though we have not been able to prove this conjecture for hypersimplices $\Delta(n, 2)$, there may be a way to extract this property from the matrix recursion presented in Proposition 4.36.

Moreover, one can count the number of monotone path according to their length (without restricting to coherent monotone paths), which amounts to counting the total number of diagonal-avoiding lattice paths. This exercise of enumerative combinatorics will be carried out in the future. Given the type of combinatorics at stake, it does not seem senseless to think that the sequence of total number of monotone paths will be log-concave, although it remains non-trivial to prove it is.

Besides, Theorem 4.24 gives a necessary criterion for a monotone path on $\Delta(n,k)$ to be coherent. We have shown that this criterion is sufficient for the case $k=2$, but computer experiments shows that is it no longer sufficient when $k \geq 3$. The encoding of monotone paths on $\Delta(n,k)$ through lattice paths on the grid $[n]^k$ seems a good framework for studying this problem further.

Last but not least, we only give here a description of the vertices of $\mathsf{M}(n,2)$, it would be of prime interest to investigate the (higher-dimensional) faces of it. A first idea to do so is to introduce a notion of adjacencies between coherent lattice paths in order to describe the edges of $\mathsf{M}(n,2)$, but the drawings this notion gives birth to are not easy to interpret. A second idea would be to use the fact that faces of the hypersimplex are again hypersimplices (of lower dimensions): one could try to "see" $\mathsf{M}(n-1,k)$ inside $\mathsf{M}(n,k)$, and recover (properties of) the face lattice of $\mathsf{M}(n,k)$ from there. A glimpse of this is depicted in Figures 59 and 60: the 5 octagons appearing in the polytope of the second figure shall be thought of as 5 copies of the octagon on the right of the first figure (but it remains hard to explain where the 16 squares come from, and how the faces fit together).